2023

Disparate Population and Holobiont Structure of Pocilloporid Corals Across the Red Sea Gradient Demonstrate Species-Specific Evolutionary Trajectories

Carol Buitrago-López

Anny Cárdenas

Benjamin C.C. Hume

Thierry Gosselin

Fabian Staubach

See next page for additional authors

Original Publication Citation

Buitrago-López, C., Cárdenas, A., Hume, B. C. C., Gosselin, T., Staubach, F., Aranda, M., Barshis, D. J., Sawall, Y., & Voolstra, C. R. (2023). Disparate population and holobiont structure of pocilloporid corals across the Red Sea gradient demonstrate species-specific evolutionary trajectories. *Molecular Ecology*, *32*(9), 2151-2173. https://doi.org/10.1111/mec.16871

Received: 22 September 2022 | Revised: 25 January 2023 | Accepted: 30 January 2023

DOI: 10.1111/mec.16871

ORIGINAL ARTICLE

MOLECULAR ECOLOGY WILEY

Disparate population and holobiont structure of pocilloporid corals across the Red Sea gradient demonstrate species-specific evolutionary trajectories

Carol Buitrago-López[1,2] | Anny Cárdenas[3,4] | Benjamin C. C. Hume[3] | Thierry Gosselin[5] | Fabian Staubach[6] | Manuel Aranda[1] | Daniel J. Barshis[7] | Yvonne Sawall[8] | Christian R. Voolstra[1,3]

[1]Red Sea Research Center, Biological and Environmental Science and Engineering Division, King Abdullah University of Science and Technology, Thuwal, Saudi Arabia

[2]Department of Environment and Sustainability, Red Sea Global, Riyadh, Saudi Arabia

[3]Department of Biology, University of Konstanz, Konstanz, Germany

[4]Department of Biology, American University, Washington, DC, USA

[5]CSIRO Marine and Atmospheric Research, Tasmania, Hobart, Australia

[6]Institute of Biology I, Department of Evolutionary Biology and Ecology, Albert-Ludwigs-University Freiburg, Freiburg, Germany

[7]Department of Biological Sciences, Old Dominion University, Norfolk, Virginia, USA

[8]Bermuda Institute of Ocean Sciences (BIOS), St. George's, Bermuda

Correspondence
Christian R. Voolstra, Department of Biology, University of Konstanz, Konstanz, Germany.
Email: christian.voolstra@uni-konstanz.de

Funding information
Deutsche Forschungsgemeinschaft, Grant/Award Number: 433042944; King Abdullah University of Science and Technology, Grant/Award Number: BaselineFunding

Handling Editor: Pim Bongaerts

Abstract

Global habitat degradation heightens the need to better understand patterns of genetic connectivity and diversity of marine biota across geographical ranges to guide conservation efforts. Corals across the Red Sea are subject to pronounced environmental differences, but studies so far suggest that animal populations are largely connected, excepting evidence for a genetic break between the northern-central and southern regions. Here, we investigated population structure and holobiont assemblage of two common pocilloporid corals, *Pocillopora verrucosa* and *Stylophora pistillata*, across the Red Sea. We found little evidence for population differentiation in *P. verrucosa*, except for the southernmost site. Conversely, *S. pistillata* exhibited a complex population structure with evidence for within-reef and regional genetic differentiation, in line with differences in their reproductive mode (*P. verrucosa* is a broadcast spawner and *S. pistillata* is a brooder). Analysis for genomic loci under positive selection identified 85 sites (18 of which were in coding sequences) that distinguished the southern *P. verrucosa* population from the remainder of the Red Sea population. By comparison, we found 128 loci (24 of which were residing in coding sequences) in *S. pistillata* with evidence for local adaptation at various sites. Functional annotation of the underlying proteins revealed putative roles in the response to stress, lipid metabolism, transport, cytoskeletal rearrangement, and ciliary function (among others). Microbial assemblages of both coral species showed pervasive association with microalgal symbionts from the genus *Symbiodinium* (former clade A) and bacteria from the genus *Endozoicomonas* that exhibited significant differences according to host genotype and environment. The disparity of population genetic and holobiont assemblage patterns even between closely related species (family Pocilloporidae) highlights the need for multispecies investigations to better understand the role of the environment in shaping evolutionary trajectories. It further emphasizes the importance of

networks of reef reserves to achieve conservation of genetic variants critical to the future survival of coral ecosystems.

KEYWORDS
adaptation, climate change, coral reef, microbiome, population genetics, population genomics, Symbiodiniaceae

1 | INTRODUCTION

Stony corals are foundational to coral reef ecosystems, the most biodiverse marine ecosystems on earth, supporting thousands of species and providing a livelihood to close to a billion people (Moberg & Folke, 1999; Spalding et al., 2017). Shallow-water corals are sessile animals that live in an obligate endosymbiosis with photosynthetic microalgae of the family Symbiodiniaceae that cover their energetic needs (LaJeunesse et al., 2018; Muscatine & Porter, 1977) alongside a myriad of other microorganisms, most notably prokaryotes, which contribute to the physiology and stress tolerance of the emergent coral holobiont (Bourne et al., 2016; Voolstra, Suggett, et al., 2021; Ziegler, Seneca, et al., 2017). Coral holobionts are fine-tuned to their prevailing environmental settings and particularly sensitive to changes in temperature or nutrient levels, which makes them vulnerable to local and global anthropogenic impact (D'Angelo & Wiedenmann, 2014; Donovan et al., 2021; Pogoreutz et al., 2017; Voolstra, Valenzuela, et al., 2021). In particular, extended periods of warming above their maximum monthly mean (MMM) summer temperatures can trigger coral bleaching, that is, the loss of the endosymbiotic Symbiodiniaceae, that often leads to subsequent coral death (Glynn, 1993; Lesser, 2011; Rädecker et al., 2021). Global coral cover has declined by about 50% since the 1950s (Eddy et al., 2021), and most coral reefs around the world are now at risk of repeat annual bleaching as a consequence of ongoing climate change (Hughes et al., 2017, 2018; Kleypas et al., 2021). Current projections estimate that between 70% and 90% of existing coral reefs are at jeopardy to disappear in the coming two decades (Allen et al., 2018; Frieler et al., 2012). This makes the protection of corals a priority and highlights the need to better understand patterns of connectivity and diversity to effectively guide conservation efforts to maximize extant genetic diversity (Zoccola et al., 2020).

Despite their overall sensitivity to environmental disturbance, corals exhibit a broad variance in their response to stress, even within a single reef, suggesting a large capacity for acclimation and adaptation, at least for some species (Dixon et al., 2015; Palumbi et al., 2014; Savary et al., 2021; Thomas et al., 2018; Voolstra et al., 2020; Voolstra, Suggett, et al., 2021; Voolstra, Valenzuela, et al., 2021). In line with that, studies found large effective population sizes and a high standing genetic diversity in coral species (Bay et al., 2017; Cooke et al., 2020; Matz et al., 2018; Prada et al., 2016; Robitzch et al., 2015). Most notably, in concordance with the increase in frequency and intensity of coral bleaching over the last decade, corals have started to bleach at significantly higher sea surface temperatures (SSTs) in the last decade (Sully et al., 2019). However, it is unclear whether this increase is caused by increased selection for more tolerant coral colonies or by acclimation. It is important to understand whether such putative directional selection reduces the genetic diversity of coral populations and the consequences it bears, e.g. with regard to disease susceptibility or coral growth (Bay & Palumbi, 2017; Bruno et al., 2007; Carricart-Ganivet et al., 2012). In order to pinpoint the effects of environmental change on population genetic diversity, it is necessary to establish baselines from which change can be measured. For the majority of coral species, such genetic diversity baselines are typically either not available or spatially restricted, although population genomic approaches can be employed to estimate current and past population sizes to infer changes in population genetic variation (Prada et al., 2016).

Coral populations of the Red Sea are subject to strong environmental gradients across their latitudinal spread with reef sites in the southern Red Sea experiencing some of the warmest maximum monthly mean (MMM) summer temperatures globally (Berumen et al., 2019; Kleinhaus et al., 2020; Osman et al., 2018; Voolstra, Valenzuela, et al., 2021). For this reason, there is a long and continuous interest in studying Red Sea coral populations, their thermal limits, and how their extraordinary thermal tolerance aligns with the prevailing environment (Evensen et al., 2021, 2022; Fine et al., 2013; Savary et al., 2021; Voolstra, Valenzuela, et al., 2021). The Red Sea is characterized by strong and opposing salinity-temperature-nutrient gradients (Berumen et al., 2019; Sawall & Al-Sofyani, 2015) in combination with oceanographic phenomena such as low tidal cycles (Sultan et al., 1995), the Arabian Monsoon (Raitsos et al., 2015), and eddies (Zhan et al., 2014), which are thought to affect larval dispersal and consequently genetic exchange (Robitzch et al., 2015; Wang et al., 2019). It is currently unclear to what extent the pronounced environmental differences across the latitudinal range of the Red Sea affect genetic variation or constrain the distribution of thermotolerant corals (Fine et al., 2013; Osman et al., 2018), with population genetic studies on reef organisms finding contrasting results. For instance, some studies on fishes and sponges support a genetic break at approximately 17–20° latitude that coincides with a marked environmental shift (Froukh & Kochzius, 2007; Giles et al., 2015; Nanninga et al., 2014; Saenz-Agudelo et al., 2015), while works on other fish species (DiBattista et al., 2020) and the giant clam *Tridacna maxima* found no evidence for such a genetic break, although associated Symbiodiniaceae of *T. maxima* differed across their latitudinal spread (Lim et al., 2020; Rossbach et al., 2021). Similarly, coral

population differentiation is inconsistent across species (Maier et al., 2005, 2009; Robitzch et al., 2015).

To establish a baseline of genetic connectivity for coral populations across the Red Sea that can inform conservation efforts and future trajectories, we characterized the population structure of two common pocilloporid corals with contrasting reproductive strategies, *Pocillopora verrucosa* (Ellis & Solander, 1786; broadcast spawner) and *Stylophora pistillata* (Esper, 1792; brooder). Using restriction-site associated DNA sequencing (RAD-Seq) (Baird et al., 2008), we assessed genetic diversity across 12° of latitude covering 1500 km of overwater distance. In addition, we determined Symbiodiniaceae and prokaryotic assemblage using ITS2 and 16S rRNA marker gene sequencing (metabarcoding), respectively, to denote how holobiont diversity aligns with host genetic diversity and the prevailing environment. Such data can assist in the identification and designation of priority areas to support effective conservation through incorporation of sites that harbor genetically distinct coral populations.

2 | MATERIALS AND METHODS

2.1 | Sample collection

Approximately finger-sized fragments of *Pocillopora verrucosa* (n = 317) and *Stylophora pistillata* (n = 448) colonies were collected at 19 reef sites from six regions (from North to South): Maqna (MAQ), Al-Wajh (WAJ), Yanbu (YAN), Thuwal (KAU), Doga (DOG), and Farasan Islands (FAR), spanning the extent of the Saudi Arabian Red Sea (~1500 km overwater distance) (Table S1). Sampling was conducted using SCUBA in September 2011 and in March 2012. The sampled colonies were collected from windward reef sites at depths between 5 and 10 m and at least 5 m apart to minimize the collection of clones. Samples were preserved in DESS buffer (Seutin et al., 1991; Voolstra et al., 2022; Voolstra, Quigley, et al., 2021), transported back to the laboratory at room temperature, and subsequently stored at −80°C until further processing (Voolstra et al., 2022).

2.2 | DNA extraction

Genomic DNA was extracted using the Qiagen DNeasy Plant mini kit (Qiagen) with minor modifications. A small fraction (5–10 mm^2) of each coral sample was excised with sterile bone clippers and placed in a 1.5 mL microtube containing 400 µL AP1 lysis buffer and 500 µL of 0.5 mm glass beads (BioSpec). Microtubes were agitated using a Qiagen TissueLyser II at 30 Hz for 90 s. Further steps were performed following the manufacturer's protocol, using a single DNA elution with 80 µL of AE buffer. DNA was quantified using the Quant-iT dsDNA high sensitivity kit (ThermoFisher) and a SpectraMax Paradigm Multi-Mode Microplate Reader (Molecular Devices) with excitation/emission set to 485 nm/535 nm.

2.3 | RAD-Seq library preparation and sequencing

RAD-Seq libraries were constructed using a single restriction enzyme protocol developed previously (Etter et al., 2011), with some modifications. Briefly, 500 ng of DNA per sample were digested with 1 µL (20 units) of the 6 bp (5′-CTGCA^G-3′) recognition enzyme PstI (NEB). This enzyme was shown to work in RAD-Seq applications targeting pocilloporid corals (Combosch & Vollmer, 2015; Smith et al., 2017). In line with this, an *in silico* digestion of the *P. verrucosa* and *S. pistillata* genomes (Buitrago-López et al., 2020; Liew et al., 2016; Voolstra et al., 2017) using SIMRAD version 0.96 (Lepais & Weir, 2014) predicted 80,718 and 80,763 restriction sites, respectively. After digestion with PstI, DNA from each sample was ligated to custom-made oligonucleotides using T4 DNA ligase that contained (in 5′→3′ direction): Illumina adapters, a six bp barcode, and a TGC*A PstI overhang (Table S1, Table S2). Ligated samples were purified using AMPURE XP beads at 1.8× the volume (Beckman Coulter). After that, equal amounts of DNA from 24 uniquely barcoded samples were combined to obtain 1 µg of DNA per pool. In total, 32 DNA pools of 24 samples each were generated and processed using the NEBNext Ultra DNA library preparation kit (NEB), according to the manufacturer's instructions (Table S1). Size selection was done by running each sequencing library on a gel with subsequent gel extraction of DNA at a target library size of 500 bp and subsequent recovery using the Zymoclean gel DNA recovery kit (Zymo Research) with an elution volume of 24 µL. The size-selected libraries were enriched in duplicate PCR reactions using 10.5 µL of gel-excised DNA as a template, 2 µL of each of the primers 5′-AATGATACGGC GACCACCG*A-3′ and 5′-CAAGCAGAAGACGGCATACG*A-3′ (asterisks denote a phosphorothioate modification to protect against endonuclease activity) at 10 µM, and 12.5 µL of the KAPA High Fidelity Master Mix (Kapa Biosystems) with a cycling profile of 95°C for 5 min, between 12–15 cycles of 98°C for 20 s, 60°C for 30 s, 72°C for 30 s, and a final extension step of 72°C for 5 min. Finally, after a cleanup step using 25 µL of AMPURE XP beads, the DNA concentration of multiplexed libraries was quantified using the high sensitivity Qubit dsDNA kit (ThermoFisher). Each of the 32 multiplexed libraries was concentrated to 10 nM and paired-end sequenced on the HiSeq2500 Illumina platform (2 × 125 bp) at the KAUST Bioscience Core Laboratory.

2.4 | Sequencing data filtering

Paired-end read quality was inspected with FASTQC version 0.11.8 (Andrews, 2010), and adapter sequences were removed using TRIMMOMATIC version 0.38 (Bolger et al., 2014). Subsequently, sequence reads were demultiplexed using the module *process_radtags* in the software STACKS version 1.48 (Catchen et al., 2013). PCR duplicates were identified and removed from further analysis using the module *clone_filter* in the software STACKS version 1.48. Remaining paired-end reads were cropped to a consistent length of 110 bp

for STACKS processing using TRIMMOMATIC version 0.38. Paired-end reads were mapped to their respective reference genomes, that is *Pocillopora verrucosa* (Buitrago-López et al., 2020) or *Stylophora pistillata* (Voolstra et al., 2017), using BOWTIE2 version 2.3.5.1 (Langmead & Salzberg, 2012) with settings for very sensitive local alignment (-D 20 -R 3 -N 0 -L 20 -i S,1,0.50); only concordant paired-end alignments were kept for subsequent analyses. BAM files were sorted according to their aligned scaffold/position using the software SAMTOOLS version 1.9 (Li et al., 2009) for use in all subsequent analyses.

2.5 | SNP calling and filtering

Catalogs of RAD loci (i.e., sequences starting or ending with a restriction enzyme site) were constructed using default settings of the reference genome-based *gstacks* module in STACKS version 2.0 (Rochette et al., 2019). *Gstacks* employs a Bayesian algorithm for discovery of biallelic single nucleotide polymorphisms (SNPs) within each RAD locus by considering all individuals for each species (*P. verrucosa* $n = 316$, *S. pistillata* $n = 448$). Each sample was then genotyped at each identified SNP position. The SNP-derived genotyping datasets were first filtered using the *populations* module in STACKS version 2.0, retaining SNPs with a minimum minor allele count (MAC) of four (--min-mac 4) present in more than 80% of all individuals per species (-R 0.8). The resulting *populations*.vcf files were imported into RADIATOR version 1.1.8 (Gosselin, 2020) and further filtered with the function *filter_rad*. For reasons of comparability, equivalent filtering thresholds were applied to datasets from both species. First, individuals with more than 20% missing (SNP-based) genotypes were discarded. After that, criteria such as MAC, sequencing coverage, and genotyping rate were used to further filter SNPs (Table S3). The remaining SNPs had a mean coverage ranging between 15× and 75× across samples, were identified in at least 90% of all samples, and had a MAC equivalent to ~1% of all alleles (*P. verrucosa* MAC = 8, *S. pistillata* MAC = 10). In addition, the overall observed heterozygosity of each sample was inspected to identify and remove outlier individuals with poor polymorphism discovery, that is, exceedingly low/high heterozygosity (see Table S3 for thresholds). Further, putative clones were filtered using a distance-based approach (see Table S3 for thresholds). Finally, SNPs with extreme deviation from the Hardy–Weinberg equilibrium (HWE p-values ≤ .0001) occurring in at least half of the sampling sites were discarded as they represent putative genotyping errors (https://rdrr.io/github/thierrygosselin/radiator/man/filter_hwe.html). Relatedness analyses were conducted for both coral species to assess the putative presence of cryptic species complexes that would confound downstream analyses as well as to identify individuals from evolutionary distinct groups for exclusion from subsequent analyses. The relatedness analyses were conducted using the function *snpgdsIBS* in SNPRELATE version 1.20.1 (Zheng et al., 2012) and visualized in the form of dendrograms using the DENDEXTEND R package (Galili, 2015). For the *P. verrucosa* dataset, the relatedness analysis identified 2 individuals belonging to the *P. verrucosa* mtORF type 7 haplotype that were discarded, while the vast majority of samples belonged to the type 3 mtORF haplotype (Pinzón et al., 2013; Schmidt-Roach et al., 2014). This is in line with a previous study using a subset of our samples that identified a very low prevalence of type 7 mtORF haplotypes of 0.3% (Monroe, 2015). For the remaining samples, there was no apparent geographical/site pattern for *Pocillopora verrucosa* (Figure S1). For *Stylophora pistillata*, the dendrogram showed a separation into two broad clusters that were further split into multiple subclusters (Figure S1). This separation did not follow any apparent geographic or site pattern (Figure S1), suggesting that putative unconsidered cryptic lineages would not confound analyses in a systematic manner (although they would affect genetic diversity analyses, Table S4). In general. *S. pistillata* exhibited a much more complex differentiation pattern with multiple sublineages of varying genetic distance, while *P. verrucosa* did not exhibit any apparent substructuring (Figure S1). Although we cannot rule out the presence of a cryptic species complex for *S. pistillata*, we considered all samples to be from a single species, in line with earlier studies (Arrigoni et al., 2016; Keshavmurthy et al., 2013; Voolstra, Valenzuela, et al., 2021). Following this, 296 samples for *P. verrucosa* and 367 samples for *S. pistillata* were available for all subsequent analyses (Table S1).

2.6 | Genetic diversity and population structure analyses

For each species, genetic diversity was assessed at the level of sampling site (i.e., reef) and region (i.e., nearby reefs) for the 296 and 367 samples for *P. verrucosa* and *S. pistillata*, respectively (see above), by determining nucleotide diversity (π), observed heterozygosity (H_O), expected heterozygosity (H_E), and inbreeding coefficient (F_{IS}). To ease computational burden, SNP data sets for both species were thinned based on their non-random association, that is, linkage disequilibrium (LD). LD between pairs of samples was measured as the squared genotypic correlation coefficient (r^2) using the RADIATOR function *filter_ld*, discarding a single SNP per comparison when $r^2 > 0.1$. We ran AMOVA (1000 permutations) as implemented in POPPR version 2.9.0 (Kamvar et al., 2014) to quantify the proportion of the genetic variance and genetic differentiation explained at the level of site and region. Genetic differentiation was estimated between pairs of sites using F_{ST}, given that AMOVA resulted in larger percentages of genetic variance being explained at the reef level. Pairwise F_{ST} values were calculated using the R package STAMPP version 1.6.1 (Pembleton et al., 2013) with 95% confidence intervals based on 1000 bootstrap replicates. Pairwise F_{ST} values were considered significantly different when they were different from zero with non-overlapping 95% confidence intervals. The correlation between geographic and genetic distance between reefs was tested using the isolation by distance (IBD) function *gl.ibd* in DARTR version 1.8.3 (Gruber et al., 2018). Population genetic structure of *P. verrucosa* and *S. pistillata* was investigated using a combination of model-free and model-based approaches. A model-free principal component analysis (PCA) was

carried out using PLINK version 1.9 (Purcell et al., 2007), and the results were visually inspected using the graphic functions in PCAVIZ version 0.3-37 (Novembre et al., 2019). An admixture model was then run using ADMIXTURE version 1.3.0 (Alexander & Lange, 2011) to infer ancestry proportions for each individual by computing maximum likelihood estimates of the underlying admixture coefficients and ancestral allele frequencies. Ten unsupervised ADMIXTURE runs with random starting seeds were performed for each number of genetic clusters (*K*) to be tested. Composite bar plots of the resulting ancestry proportions were generated with PONG version 1.4.9 (Behr et al., 2016) that also estimates a similarity metric between runs to assess convergence. To evaluate relationships between the inferred genetic populations, we computed a scaled covariance matrix of population allele frequencies based on non-admixed individuals (i.e., ≥0.9 probability of assignment to one of the *K* clusters) using the software BAYPASS version 2.2 (Gautier, 2015).

2.7 | ITS2 amplification, sequencing, analysis

Internal transcribed spacer 2 (ITS2) amplicon libraries of 764 samples (317 *P. verrucosa*, 447 *S. pistillata*) and 2 negative controls (no template PCRs) were constructed to investigate the diversity of the Symbiodiniaceae community of *P. verrucosa* and *S. pistillata* samples. The ITS2 region of the rRNA gene array was amplified using the primers SYM_VAR_5.8S2 [5′-TCGTCGGCAGCGTCAGATGTGTATAAGAGACAGGAATTGCAGAACTCCGTGAACC-3′] and SYM_VAR_REV [5′-GTCTCGTGGGCTCGGAGATGTGTATAAGAGACAGCGGGTTCWCTTGTYTGACTTCATGC-3′] (Hume et al., 2013, 2015, 2018) with the corresponding Illumina adaptor overhangs underlined. For each sample, triplicate PCRs were run using ~50 ng of DNA and the Qiagen Multiplex PCR kit in volume reactions of 10 μL with a final primer concentration of 0.5 μM. The thermal cycling conditions were 95°C for 15 min, 30 cycles of 95°C for 30 s, 56°C for 90 s, and 72°C for 30 s, followed by a final extension step of 72°C for 10 min. Triplicate PCR products for each sample were pooled following confirmation of ITS2 amplification by gel electrophoresis. Pooled PCR products from each sample were cleaned using ExoProStar 1-step (GE Healthcare). Pooled PCR products were indexed using the 384 Nextera XT Index Kit version 2 (dual indexes and Illumina sequencing adaptors added) with a second PCR using eight cycles and the same amplification conditions as above. Successful addition of barcodes was checked by the larger size of the PCR products on a 1% agarose gel. PCR products were pooled in equimolar DNA concentrations using the SequalPrep Normalization Plate Kit (Invitrogen). Subsequently, 4 μL (25 ng of DNA) of each sample were pooled in a 1.5 mL microtube and concentrated with a CentriVap Benchtop Vacuum Concentrator (Labconco). The two sequencing libraries were quality checked using the Agilent High Sensitivity DNA Kit on the Agilent 2100 Bioanalyzer (Agilent Technologies) and quantified using the qPCR KAPA Library Quantification kits (Roche). ITS2 libraries were sequenced at 2 nM DNA using 20% of PhiX on the Illumina MiSeq platform (2 × 301 bp) with the V3 chemistry according to the manufacturer's instructions.

Demultiplexed paired-end sequencing files were submitted to the SymPortal (Hume et al., 2019) framework (https://symportal.org/), where sequence reads were processed using a MOTHUR-based pipeline (Schloss et al., 2009), taxonomically screened using BLAST with a SymPortal-curated Symbiodiniaceae database, and finally decomposed using minimum entropy decomposition (MED) (Eren et al., 2015). SymPortal predicts ITS2 type profiles (Davies et al., 2022) as a proxy for putative Symbiodiniaceae taxa by identifying sets of sequences, referred to as defining intragenomic sequence variants (DIVs), found in common between multiple samples. Profiles recovered from *P. verrucosa* had a larger number of DIVs in common with their next most similar profile than in *S. pistillata* (3.50 vs. 2.01 DIVs in common for *P. verrucosa* and *S. pistillata*, respectively). As such, comparing profile richness between the two corals would be analogous to comparing richness at different taxonomic levels (i.e., comparing the number of subspecies in *P. verrucosa* to the number of species in *S. pistillata*). To homogenize the degree of dissimilarity between predicted profiles in both coral species and to make the comparison of profile richness a better proxy of Symbiodiniaceae species richness, we clustered highly similar profiles (i.e., ≥3 DIVs in common) into representative profiles defined by the common DIVs. In the remainder of the manuscript, when referring to profiles, it is these representative profiles (i.e., post clustering) that we are referring to. Clustered and non-clustered profile count tables are provided in the associated GitHub repository (https://github.com/reefgenomics/Red-Sea-RADSeq). To visualize the distribution of putative Symbiodiniaceae taxa across the sampled sites, we plotted profiles for all samples that passed RAD-Seq filtering, that is, 296 for *P. verrucosa* and 367 for *S. pistillata* (see above).

To test for correlation of host genotype (based on genetic cluster assignment K; see above) and environmental condition (i.e., maximum monthly mean MMM sea surface temperatures based on reef locations and factorized into 1°C levels, Table S5) on ITS2 assemblage structure and ITS2 beta diversity variation, we generated PCoA plots and ran PERMANOVA analyses. MMMs were obtained from NOAA's Coral Reef Watch (CRW) using the climatology database (ftp://ftp.star.nesdis.noaa.gov/pub/sod/mecb/crw/data/5km/v3.1_op/climatology/nc/) queried with cwsample, which is part of the NOAA CoastWatch Utilities (Liu et al., 2014). Consequently, *sensu stricto* we tested for differences among thermal regimes (as indicated by different MMMs). Given that environmental variables such as temperature, salinity, and nutrients correlate across the latitudinal gradient of the Red Sea and thus cannot be disentangled from each other (Berumen et al., 2019; Ngugi et al., 2012; Sawall et al., 2015), we posited that differences in temperature are representative of environmental differences, although actual environmental regimes were not accounted for in the analysis. To compute the required between-sample dissimilarity matrices (one per coral genus), we generated Bray–Curtis distances using square-root transformed post-MED sequence counts (output by SymPortal) only for samples that could be confidently

assigned to a coral host genetic population/cluster (i.e., ≥0.9 probability of assignment to one of the *K* clusters; see above) and only for the *Symbiodinium* sequences (due to the lack of abundance of other Symbiodiniaceae genera) resulting in 202 and 281 samples for *P. verrucosa* and *S. pistillata*, respectively. Due to an imbalanced design (i.e., different numbers of samples per genetic cluster or temperature category), we tested for a significant difference in dispersion between genetic clusters and MMM using the R *betadisper* function (a significant difference in dispersion may affect the power and accuracy of the PERMANOVA test) (Anderson & Walsh, 2013). Due to the additive nature of the PERMANOVA modelling, we assessed for overlap in apportioning of variance by running PERMANOVAs with the independent variables in alternating orders. The R and python scripts used to generate figures and run statistics, as well as the input count tables are deposited in the associated GitHub repository (https://github.com/reefgenomics/Red-Sea-RADSeq).

2.8 | 16S amplification, sequencing, analysis

16S rRNA gene amplicon libraries of 764 samples (317 *P. verrucosa*, 447 *S. pistillata*) and 2 negative controls (no template PCRs) were constructed to assess prokaryotic diversity. PCR amplification was done using primers targeting the hypervariable regions V5–V6 of the 16S rRNA gene. Sample-based PCRs were done in triplicates using primers 784F [5′-TCGTCGGCAGCGTCAGATGTGTATAAGAGACAGAGGATTAGATACCCTGGTA-3′] and 1061R [5′-GTCTCGTGGGCTCGGAGATGTGTATAAGAGACAGCRRCACGAGCTGACGAC-3′] (Andersson et al., 2008; Bayer et al., 2013) with Illumina universal adaptors (underlined) with the following conditions: 95°C for 15 min, followed by 27 cycles of 95°C for 30 s, 55°C for 90 s, 72°C for 30 s, and a final extension step of 72°C for 10 min. Further steps in the library preparation are identical to those described for the ITS2 library preparation (see above). Briefly, triplicated PCRs from each sample were pooled, cleaned with ExoProStar 1-step (GE Healthcare), and used as template for a second PCR amplification to attach Illumina Nextera barcodes using eight cycles. Successful addition of barcodes was checked by the larger size of the PCR products on a 1% agarose gel. PCR products were pooled in equimolar DNA concentrations using the SequalPrep Normalization Plate Kit (Invitrogen) and concentrated using the CentriVap Benchtop Vacuum Concentrator (Labconco). The final libraries were assessed using a Bioanalyzer 2100 (Agilent) and quantified using the qPCR Kapa Library Quantification kit (KAPA Biosystems). The 16S rRNA gene amplicon libraries were sequenced at 2 nM DNA using 20% PhiX on the Illumina MiSeq platform using the 2 × 301 bp V3 chemistry according to the manufacturer's specifications.

Demultiplexed paired-end sequencing files were used to infer prokaryotic 16S rRNA gene amplicon sequence variants (ASVs) using DADA2 (Callahan et al., 2016). First, forward and reverse reads were trimmed to 245 and 220 bp, respectively, based on quality profiles. Reads were truncated at the first instance of a quality score ≤10, and reads with an expected error >2 or with the presence of ambiguous bases were discarded. Error rate was estimated from 215,022,045 total bases in 924,826 reads from the first three samples using the DADA2 algorithm. After merging paired-end reads and removing chimeric sequences, 45,374 ASVs were inferred from 766 samples (317 *P. verrucosa*, 447 *S. pistillata*, 2 negative controls).

Taxonomy was assigned to ASVs using the SILVA database (version 138) (Quast et al., 2013). ASV relative abundance tables are provided in the associated GitHub repository (https://github.com/reefgenomics/Red-Sea-RADSeq). A total of 110 ASVs were determined to be putative contaminants based on their presence in negative controls and consequently removed from all samples. An ASV was considered a contaminant if the ratio of its mean relative abundance across negative controls over its mean relative abundance across all samples was >0.1 (i.e., 10% of sequenced reads). Only samples from coral colonies that passed RAD-Seq filtering (see above) and those with more than 1000 read pairs were displayed in bar plots to represent the top 20 most abundant bacterial ASVs (*P. verrucosa* $n = 296$, *S. pistillata* $n = 364$). As for the ITS2 analysis, further analyses were done on samples that could be assigned to a single coral host genetic population/cluster with ≥0.9 probability of assignment to one of the *K* genetic clusters (see above), resulting in datasets of 203 *P. verrucosa* and 309 *S. pistillata* samples, respectively. Beta diversity was calculated using the Bray–Curtis dissimilarity index from relative abundances using the *vegdist* function from the R package VEGAN version 2.5-7 (Oksanen et al., 2007). Differences in bacterial beta diversity were calculated using PERMANOVA among host genetic clusters *K* and environmental conditions (i.e., regional MMMs) (see above) using the *adonis* function implemented in VEGAN using 999 permutations. Since significant PERMANOVAs may indicate either a change in the bacterial community composition by groups (i.e., host genetic cluster or MMM) or heterogeneity of group dispersion, the betadisper function implemented in VEGAN was used to assess whether beta-diversity differences were driven by changes in dispersal. Beta diversity was visualized on a principal coordinate analysis (PCoA) using PHYLOSEQ version 1.34.0 (McMurdie & Holmes, 2013). Indicator species analysis was performed with the *multipatt* function of the INDICSPECIES package (De Cáceres & Legendre, 2009) using 1000 permutations, and results were plotted using the UPSETR package (Conway et al., 2017). Alpha diversity was calculated using the Shannon–Weaver index using the diversity function implemented in VEGAN on rarefied ASV abundances, given the large differences in sequencing depth between samples. Abundances were rarefied to the lowest count values across the dataset (both coral species), corresponding to 1018, and overall differences in alpha diversity across host genetic clusters and regional temperatures (i.e., MMMs) were tested using Kruskal–Wallis tests. R scripts used to generate figures, run statistics, and input count tables are available in the associated GitHub repository (https://github.com/reefgenomics/Red-Sea-RADSeq).

2.9 | Linkage disequilibrium (LD) analysis

To assess whether differences in reproductive strategies (*P. verrucosa* is a broadcast spawner with external fertilization, *S. pistillata* is a brooder with internal fertilization) align with differences in LD, we examined LD decay as a proxy for the non-random association of alleles (SNPs) at different loci. We only considered colonies with a probability of assignment ≥0.9 (i.e., non-admixed) to a genetic cluster ($K = 2$ for 203 *P. verrucosa* samples; $K = 6$ for 312 *S. pistillata* samples, see above). LD was estimated based on loci within the ten largest scaffolds from the genome assemblies of each species. Pairwise LD within each scaffold was computed as the squared genotypic correlation coefficient (r^2) using PLINK version 1.9 considering all determined SNPs with a minor allele frequency (MAF) greater than 5%. LD decay was visually inspected by plotting the mean r^2 in bins of 100 bp. R scripts used to generate figures and run statistics are available in the associated GitHub repository (https://github.com/reefgenomics/Red-Sea-RADSeq).

2.10 | Candidate loci under selection

To identify candidate loci under selection between the genetic clusters of each species ($K = 2$ for 203 *P. verrucosa* samples; $K = 6$ for 312 *S. pistillata* samples; see above), we employed BAYESCAN version 2.0 (Foll & Gaggiotti, 2008) and BAYPASS version 2.2 (Gautier, 2015). The analyses were based on the same set of unlinked SNPs used for the population structure assessment (see above), with only non-admixed individuals being considered (i.e., ≥0.9 probability of assignment to one of the *K* clusters). For BAYESCAN, three Markov chain Monte Carlo (MCMC) runs were done with default parameters after 50 pilot runs, a thinning interval size of 20, and prior odds for the neutral model of 100, 500, and 1000, respectively. Candidate SNPs under positive selection were selected at a 5% false discovery rate (FDR), subsequently evidence strength associated with each candidate loci was assessed using the Bayes Factor scale (Jeffreys, 1939). Although the positively selected SNP candidates largely overlapped between the different runs, subsequent analyses were carried out on the SNP candidates using prior odds of 100 for the neutral model to increase statistical power. For BAYPASS, three independent runs were done to determine proper convergence of MCMCs by means of the distance between the resulting covariate matrices using the R function *fmd.dist* (Gautier, 2015). The distribution of the *p*-values associated with XtX (i.e., F_{ST}-like statistics corrected for the neutral structuring across a population) for each locus proved inadequate for FDR correction. Therefore, we performed a calibration using a pseudo-observed dataset (POD), as recommended (Gautier, 2015). For our POD, 100,000 SNPs were simulated with the R function *simulate.baypass* (Gautier, 2015) incorporating the Omega matrix and the Pi Beta distribution obtained from the real data. The simulated POD was used as input for BAYPASS, which was run using default settings. The resulting Omega matrix was compared to the one estimated with the actual data to ensure reproducibility. Candidate outlier SNPs were identified by comparing the posterior mean of the XtX statistic obtained with the POD and real data, setting a threshold of 99.9% for the candidates under positive selection. Finally, candidate loci discovered through both approaches were annotated using SNPEFF version 4.2 (Cingolani, Platts, et al., 2012) to annotate and predict the effects of genetic variants (e.g., amino acid change in the coding sequence of a gene) based on reference genome information. Databases for the genomes of *P. verrucosa* and *S. pistillata* were created based on the fasta and gff3 files downloaded from http://pver.reefgenomics.org/ and http://spis.reefgenomics.org/ (Liew et al., 2016). SNPEFF was run with default settings, and the resulting annotation was filtered using the perl script *vcfEffOnePerLine.pl* and the software SNPSIFT version 4.2. (Cingolani, Patel, et al., 2012). We only considered SNPs that mapped to annotated genes or were within 1 kb up- or downstream of an annotated gene. The list of candidate genes was further analysed using PANTHER (Mi et al., 2019) at the level of protein classes.

3 | RESULTS

3.1 | Comprehensive genetic representation of *P. verrucosa* and *S. pistillata* by RAD-Seq loci

We sampled corals across >1500 km of the Saudi Arabian Red Sea to assess population structure of the corals *P. verrucosa* and *S. pistillata* (Figure 1a, Table S1). We collected samples from 317 *P. verrucosa* and 448 *S. pistillata* colonies from 19 reefs across 12 degrees of latitude (from 16° to 28°) and genotyped them using a RAD-Seq approach. Sequencing of the RAD-Seq libraries resulted in an average of ~7 million read pairs for 764 of the samples (excepting 1 failed sample from *P. verrucosa* PFAR-R3-10, Table S1). Our sequencing effort allowed us to assemble 878,169 RAD-Seq loci for *P. verrucosa* (mean length = 276.44 bp, SD = 52.1 bp; mean coverage = 21.8×, SD = 8.9×) and 2,160,581 RAD-Seq loci for *S. pistillata* (mean length = 322.76 bp, SD = 107.78 bp; mean coverage = 14.9×, SD = 11.0×). After filtering, 296 samples of *P. verrucosa* (93.67%) were genotyped at 69,457 RAD-Seq loci (mean length = 411.93 bp, SD = 26.87 bp; mean coverage = 20.76×, SD = 4.57×; mean no. of SNPs per locus = 5.28, SD = 4.58) and 367 samples of *S. pistillata* (81.91%) were genotyped at 58,658 RAD loci (mean length = 497.15 bp, SD = 21.03 bp; mean coverage = 20.77×, SD = 4.57×; mean no. of SNPs per locus = 4.89, SD = 3.08) (see Table S3 for detailed output after each filtering step). The proportion of missing genotypes per individual in the resulting datasets was low for both species (*P. verrucosa* min = 1.30%, max = 7.63%; *S. pistillata* min = 1.11%, max = 3.16%), falling within ranges that enable reliable population genomics inferences (Chattopadhyay et al., 2014). Overall, recovered RAD-Seq loci for both coral species covered equivalent proportions (~7%) of their total genome size.

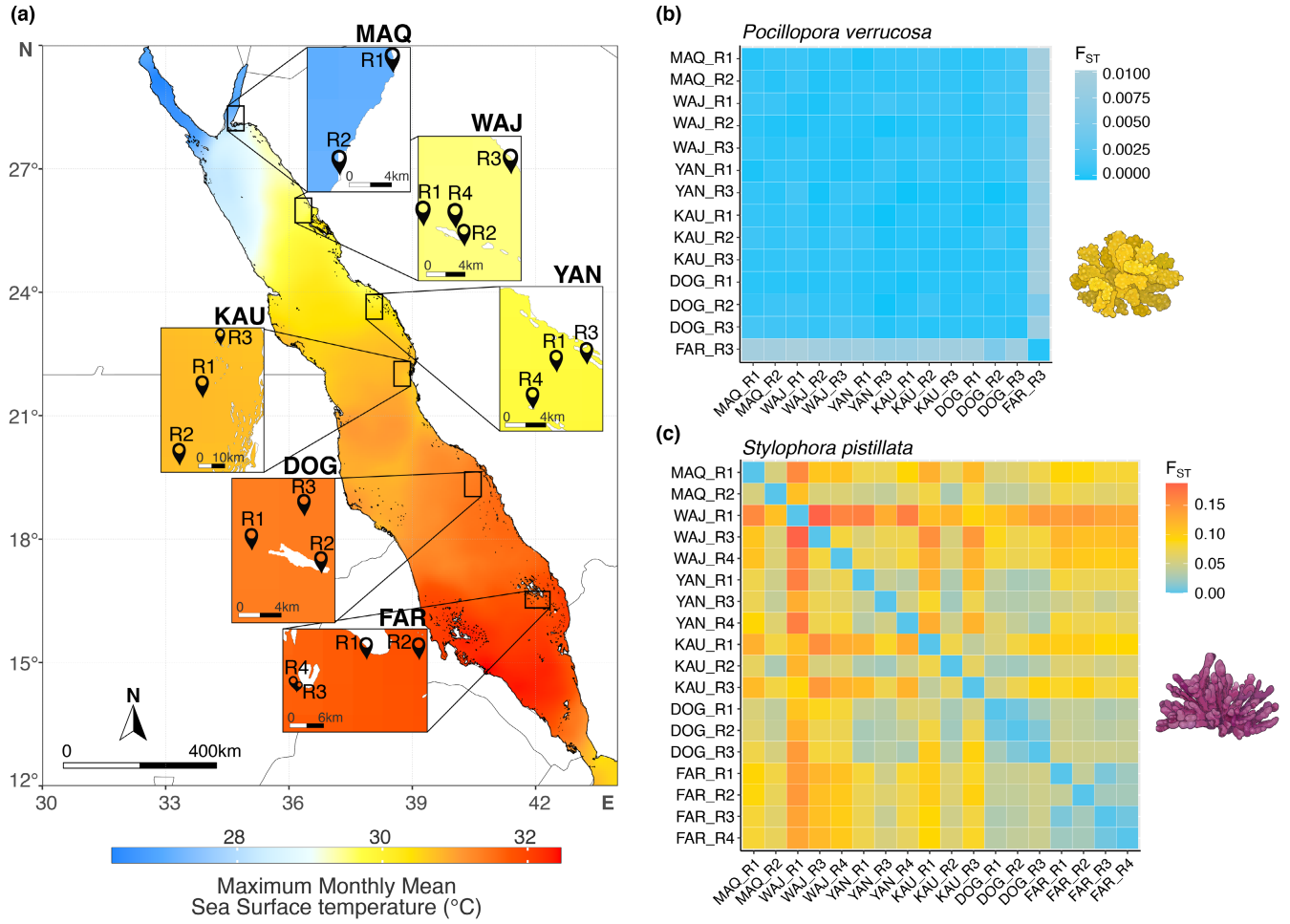

FIGURE 1 Sampling locations and genetic differentiation of *Pocillopora verrucosa* and *Stylophora pistillata* populations in the Red Sea. (a) Map of the Red Sea. Insets indicate the location of each of the 19 sampled reef sites. Colour scale of the maximum monthly mean (MMM) sea surface temperature based on the NOAA Coral Reef Watch climatology data (Liu et al., 2014). (b, c) Heatmaps of pairwise genetic differentiation (F_{ST}) between reef sites ordered from north (top) to south (bottom) for (b) *P. verrucosa* and (c) *S. pistillata*. The colour scale associated with the F_{ST} value is on the right-hand side of the heatmap for each species.

3.2 | Contrasting patterns of genetic diversity and differentiation across populations of *P. verrucosa* and *S. pistillata*

Genetic diversity (i.e., nucleotide diversity and heterozygosity) was almost twice as high in *P. verrucosa* ($\pi = 2.56\times10^{-3}$, SD = 1.47×10^{-5}; $H_E = 1.95\times10^{-1}$, SD = 2.17×10^{-3}) than in *S. pistillata* ($\pi = 1.10\times10^{-3}$, SD = 1.23×10^{-4}; $H_E = 1.08\times10^{-1}$, SD = 1.33×10^{-2}). Accordingly, the inbreeding coefficient (F_{IS}; deviation from the HWE) was substantially lower in *P. verrucosa* ($F_{IS} = 3.80\times10^{-2}$, SD = 5.91×10^{-3}0.011) than in *S. pistillata* ($F_{IS} = 1.05\times10^{-1}$, SD = 4.32×10^{-2}). Private alleles (P_A, i.e., alleles only present in a single reef) were absent in all *P. verrucosa* reef sites, except for the southernmost reef in the Farasan Islands (FAR_R3: $P_A = 8$). By comparison, P_A were found in almost all *S. pistillata* reef sites, ranging from 2 (DOG_R3) to 564 for a reef in the Al Wajh region (WAJ_R4), located north-central (Table S4). Overall, genetic diversity was uniformly distributed along the latitudinal extent for both species.

To further explore how the genetic variance in *P. verrucosa* and *S. pistillata* was partitioned across hierarchical levels including individual, reef, and region, we conducted a hierarchical AMOVA on LD-pruned SNP data sets (*P. verrucosa* = 35,208 SNPs; *S. pistillata* = 25,318 SNPs) to reduce computational burden and maximize independence between SNPs. Although the majority of genetic variance was contained within individual coral colonies (*P. verrucosa* = 99.68%, *S. pistillata* = 87.59%, p-value < .001), some portion of the genetic variance was evident at the reef level (i.e., sampling site), and this portion was substantially higher for *S. pistillata* (*P. verrucosa* = 0.03%, p-value = .041; *S. pistillata* = 8.10%, p-value < .001; Tables S6 and S7), suggesting some degree of genetic differentiation among reefs. The genetic variance explained by region was only significant in *S. pistillata* and lower than the variance explained by reef (4.29%, p-value < .001). Overall, the genetic differentiation between reefs was much lower in *P. verrucosa* (AMOVA $F_{ST} = 0.0031$) than in *S. pistillata* (AMOVA $F_{ST} = 0.1240$). This was confirmed by pairwise F_{ST} comparisons between reefs, where only *P. verrucosa* genotypes from the southernmost reef (FAR_R3) were significantly different from

the remainder of the reefs (F_{ST} =0.005–0.01) (Figure 1b; Table S8). By contrast, *S. pistillata* exhibited significant genetic differences between all pairwise reef comparisons (Figure 1c; Table S9).

Pairwise F_{ST} among reefs in *S. pistillata* ranged from 0.006 to 0.188 with WAJ_R1 attaining the highest score (mean pairwise F_{ST} =0.138), indicating it as the genetically most distinct reef (Figure 1c; Table S9). Notably, *S. pistillata* colonies from the southern Red Sea covering the regions of DOG (DOG_R1, DOG_R2, DOG_R3) and FAR (FAR_R1, FAR_R2, FAR_R3, FAR_R4) exhibited the highest between-reefs similarity (i.e., lowest F_{ST} values), which is not the case for the reefs in the central and northern regions (Figure 1c). Weak signatures of isolation by distance (IBD) were detected in *P. verrucosa* (r_m =0.278, *p*-value = .003) and *S. pistillata* (r_m =0.238, *p*-value = .001), where only about 5.6% and 7.7% of the genetic divergence was explained by the geographic distance in *P. verrucosa* and *S. pistillata*, respectively.

3.3 | Highly connected populations of *P. verrucosa* in the Red Sea contrasts a complex population structure in *S. pistillata*

We used PCA and ADMIXTURE to assess whether Red Sea coral populations are genetically structured across their latitudinal range and the putative number of genetically distinct populations. Signatures of population genetic structure were identified in both species (*P. verrucosa n* = 296; *S. pistillata n* = 367), with concordant results between PCA and ADMIXTURE (Figure 2; Figures S2, S3). Population genetic structure as well as the number of putative ancestral populations were strikingly different between *P. verrucosa* and *S. pistillata*. For *P. verrucosa*, the large majority of individuals clustered together and exhibited extensive connectivity across the majority of the Red Sea, with the exception of (some) individuals from DOG-R2 and FAR-R3 (Figure 2a; Figure S2A,B). In line with this, two populations were inferred that exhibited marginal levels of admixture in *P. verrucosa*, one that was only present in the far South and one that comprised the majority of specimens and was distributed all across the Red Sea (*K* = 2; Figure 2a; Figure S3A). In contrast, individuals of *S. pistillata* showed complex PCA clustering patterns suggesting substructure at most reef sites (Figure 2b; Figure S2C,D). ADMIXTURE analysis corroborated the among-reefs substructure in *S. pistillata*, showing subtle admixture between six genetically distinct populations that were distributed across the Red Sea (*K* = 6; Figure 2b; Figure S3B). Although the inferred populations were not restricted to a particular region, some intricate patterning along the north-south gradient could be observed. For instance, SCL5 was only present in the South, while SCL2 and SCL6 were only present in the Central and Northern Red Sea. Further, individuals of the genetic population SCL4 could be found in most regions, while SCL3 was only found in the far south and far north locations (Figure 2b). Thus, the pattern of a distinct southern population as observed in *P. verrucosa* (which was also found in other population genetic studies) was not present in *S. pistillata*. The relationship among *S. pistillata* populations inferred from the covariance matrix of population allele frequencies indicated that SCL2 and SCL6 that predominantly occur in the central and northern Red Sea were the most divergent populations, whereas all other populations were more closely related to each other (Figure S4).

3.4 | Microbial diversity patterns are structured by host genotype and environmental regime

Assemblages of Symbiodiniaceae and prokaryotes were characterized using ITS2 and 16S rRNA amplicon sequencing. We identified a total of 62 distinct ITS2 profiles, of which only 6 were shared between *P. verrucosa* and *S. pistillata* (Figures S5 and S6). The number of distinct ITS2 profiles (post-clustering) for the 296 and 367 samples for *P. verrucosa* and *S. pistillata* with RADSeq data, respectively, indicated a lower Symbiodiniaceae richness in *P. verrucosa* (*n* = 19) than in *S. pistillata* (*n* = 49) (Figure 2, Figure S5). Considering only the six most prevalent profiles in each coral species (Figure 2), Simpson's indices (i.e., the probability that two samples picked at random will have the same most abundant ITS2 profile) for *P. verrucosa* and *S. pistillata* were 0.477 and 0.054, respectively, indicating a much more consistent association in *P. verrucosa*, in line with previous studies (Sawall et al., 2015; Voolstra, Valenzuela, et al., 2021; Ziegler, Arif, et al., 2017). Of note, two of the six most prevalent profiles of *P. verrucosa* (A1-A1c-A1h and A1-A1bv-A1cb) were found in 83% of the samples. Yet, these profiles exhibited regional differences. While A1-A1c-A1h was common across the Red Sea, the A1-A1bv-A1cb profile was particularly dominant in the southernmost reef (FAR-R3) where it was present in all sampled corals. Interestingly, Symbiodiniaceae association of *P. verrucosa* from the northernmost reef sites (i.e., MAQ-R1 and MAQ-R2) were highly variable. By contrast, the two most prevalent profiles in *S. pistillata* overall were only found in 11% of the *S. pistillata* samples but were not the predominant profiles at any of the sampled reefs. In line with the complex host genetic population structure, Symbiodiniaceae association of *S. pistillata* was variable and heterogenous with some indication of regional prevalence (see below). In both coral species, the majority of samples were associated with a single Symbiodiniaceae taxon, that is, hosted a single ITS2 profile (88% and 86% of samples in *P. verrucosa* and *S. pistillata*, respectively). However, samples in the northern-most region (MAQ) showed a greater within-sample profile richness and usually were associated with >1 ITS2 profile, often from different Symbiodiniaceae genera (51% and 58% of samples from the MAQ region were associated with >1 Symbiodiniaceae genus in *P. verrucosa* and *S. pistillata*, respectively). Both coral species showed a prevalent association with species in the genus *Symbiodinium* (84% and 77% of *P. verrucosa* and *S. pistillata* samples, respectively), yet members of *Cladocopium* were also common (15% and 21% of *P. verrucosa* and *S. pistillata* samples, respectively), particularly in the reef YAN-R1 in *S. pistillata* (Figure 2b).

For the prokaryotic community, we identified 45,264 distinct 16S rRNA amplicon sequence variants (ASVs) across all samples,

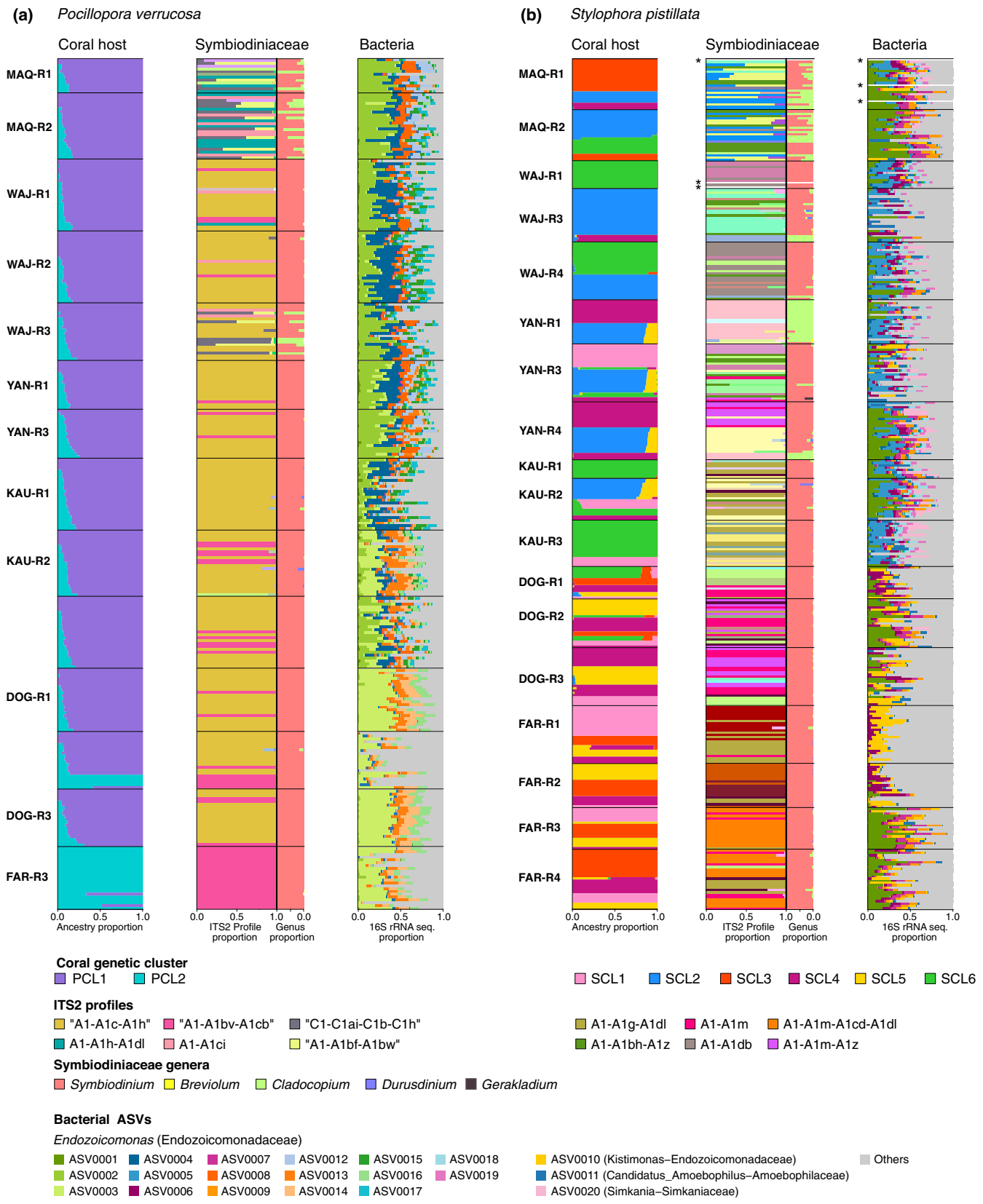

FIGURE 2 Genetic characterization of pocilloporid coral holobionts in the Red Sea. Barplots depict the population genetic structure of the coral host (left column), Symbiodiniaceae assemblage (middle column), and prokaryotic diversity (right column) of (a) *P. verrucosa* ($n = 296$) and (b) *S. pistillata* ($n = 367$) across six regions of the Red Sea (MAQ, WAJ, YAN, KAU, DOG FAR). Each horizontal bar represents an individual colony. Sampled reef sites are indicated on the left and ordered from North to South (see Figure 1). The colors indicate the ancestry proportion to each genetic cluster inferred by ADMIXTURE in *P. verrucosa* ($K = 2$; PCL1, PCL2) and *S. pistillata* ($K = 6$; SCL1-SCL6) (left columns), the six most prevalent ITS2 profiles per coral species (middle columns), and the 20 most abundant prokaryotic ASVs (right columns). Remaining ASVs are binned into the "Others" category. Asterisks indicate samples with unavailable ITS2 or 16S rRNA gene amplicon data.

representing 493 bacterial families and 1,429 genera. At large, bacterial alpha diversity was significantly higher in *S. pistillata* (Shannon = 3.09, Chao1 = 4,743) than in *P. verrucosa* (Shannon = 2.85, Chao1 = 3,879), with northern reefs being overall less diverse in both species (Figures S7 and S8). Furthermore, bacterial alpha diversity differed significantly between host genetic clusters, with PCL2 being more diverse than PCL1 for *P. verrucosa* and SCL2 and SCL3 being the least diverse of all genetic clusters in *S. pistillata* (Figure S8). We could corroborate the known prevalent association with *Endozoicomonas* of *P. verrucosa* and *S. pistillata* in the Red Sea (Bayer et al., 2013; Neave et al., 2019; Neave, Rachmawati, et al., 2017). Sequences affiliated to the genus *Endozoicomonas*, family *Endozoicomonadaceae*, represented the vast majority of the bacterial community in both species (on average 83.4% of the total community in *P. verrucosa* and 59.1% in *S. pistillata*). Interestingly, members of the *Kistimonas*, which also belong to the *Endozoicomonadaceae* family, made up a considerable proportion of the bacterial community of *S. pistillata* in the southern regions (on average 31.13%). Overall, 17 of the 20 most abundant ASVs were Endozoicomonadaceae, which were coral host-specific and more diverse in *S. pistillata* (Shannon = 2.23) than in *P. verrucosa* (Shannon = 1.90) (Figure 2, Figure S9).

To further elucidate how microbial assemblages, i.e., Symbiodiniaceae and prokaryotes, are potentially structured by host genotype (i.e., genetic cluster) and prevailing environment (i.e., temperature regime based on MMMs), we conducted PCoA ordinations and PERMANOVA analyses. Betadisper tests for significant differences in dispersions between host genotype (2 genetic clusters for *P. verrucosa*, 6 genetic clusters for *S. pistillata*) and MMM (4 temperature regimes, Table S4, S5) returned significant results ($Pr(>F) < 0.05$) for all tests for Symbiodiniaceae and prokaryote assemblages for both host species with the exception of Symbiodiniaceae temperature dispersion in *S. pistillata* (Tables S10–S15). Group levels of host genotype and MMM with larger sample numbers generally had larger dispersions, meaning that our PERMANOVAs had a reduced power to detect a significant result. Despite this reduced power, significant results were obtained ($Pr(>F) < 0.001$) for all independent variables, and interactions (where present), for both host species. These results suggest that host genotype and prevailing environment shape Symbiodiniaceae and prokaryotic assemblages, although a causal link cannot be drawn based on our data (Dubé et al., 2021; Rossbach et al., 2021). Notably, the apportioned variance of the PERMANOVA analyses to each of the independent variables was dependent on their order in the model (significant differences in dispersions between group levels hindered an exact quantitative comparison). Thus, host genotype and temperature covary and may contribute to Symbiodiniaceae and prokaryotic assemblage. PCoA ordinations supported our PERMANOVA results by showing clustering of microbial assemblages by host genetic cluster and temperature regime (Figure 3). Moreover, prokaryotic assemblage of corals exposed to the warmest temperatures (i.e., the southernmost reefs) differed from other regions (Figure 3b,d). Consequently, corals predominantly found in warmer reefs had distinct bacterial communities, as evidenced by an overall separation of genetic cluster PCL1 from PCL2 (southernmost) in *P. verrucosa* and a separation of genetic clusters SCL1, SCL3, SCL4, and SCL5 (predominant in the south) from SCL2 and SCL6 (predominant in the north-central region) in *S. pistillata*. To further explore such patterns, we identified ASVs indicative of host genetic cluster and temperature regime (Figures S10 and S11). Both coral species exhibited a suite of ASVs indicative of host genetic cluster with the common notion that host genetic clusters prevalent in the warmest regions, that is, PCL2 in *P. verrucosa* and SCL1, SCL3, SCL4, and SCL5 in *S. pistillata*, had the largest number of indicator ASVs. These indicator taxa were predominantly represented by ASVs affiliated to Flavobacteriaceae, Rhodobacteraceae, and Endozoicomonadaceae in both coral species (Figures S10 and S11; Table S16).

3.5 | Distinct signatures of linkage disequilibrium and candidate genes for positive selection in *P. verrucosa* and *S. pistillata* populations of the Red Sea

We assessed the extent of linkage between SNPs to inform haplotype length and adaptively evolving gene inference. We investigated the decay of SNP linkage as a function of the physical distance between SNPs in the 10 largest scaffolds of each species' genome. Analyses of LD for each genetically distinct population *K* of *P. verrucosa* and *S. pistillata* only included non-admixed individuals (i.e., ≥90% assignment to a genetic cluster; *P. verrucosa* = 203 colonies and *S. pistillata* = 312 colonies) genotyped at SNPs with MAF > 5% (*P. verrucosa* ~13,883.5 SNPs/population; *S. pistillata* ~7034 SNPs/population). Overall, LD decayed faster in *P. verrucosa* than in *S. pistillata* (Figure 4a), as expected from the mode of reproduction (spawning corals presumably exhibit a higher rate of sexual outcrossing than brooding corals). LD also differed between populations for both coral species. In *P. verrucosa* the largest genetic population cluster PCL1 showed a steady decay with a mean r^2 falling below .05 after approximately 15.4 kb, while r^2 did not drop below 0.05 in PCL2 (Figure 4b). Likewise, *S. pistillata* populations showed varying degrees of LD decay, with cluster SCL6 maintaining the highest LD (mean r^2 ~0.1) beyond ~100 kb (Figure 4c). In the remaining populations (genetic clusters), the mean r^2 dropped below 0.1 after about 50 kb but did not reach values lower than 0.05, with the exception of SCL2 where r^2 fell below 0.05 at about 100 kb. Notably, although the average LD for some genetic clusters is lower in *S. pistillata* than *P. verrucosa* (Figure 4b,c), each genetic cluster of *S. pistillata* exhibits greater variability (spread of each mean r^2 in 100 bp bins) than *P .verrucosa*. Consequently, the average LD decay of populations for both coral species showed a consistent trend, with *P. verrucosa* showing a faster decay (mean $r^2 < .05$ after about 25 kb) than *S. pistillata* (mean $r^2 > .05$ after about 300 kb, the size of the largest scaffolds).

Given that the Bayesian models used to identify candidate SNPs for positive/diversifying selection assume discrete populations (i.e., cannot account for substructure or admixture), we conducted the selection analyses on non-admixed individuals that could be clearly

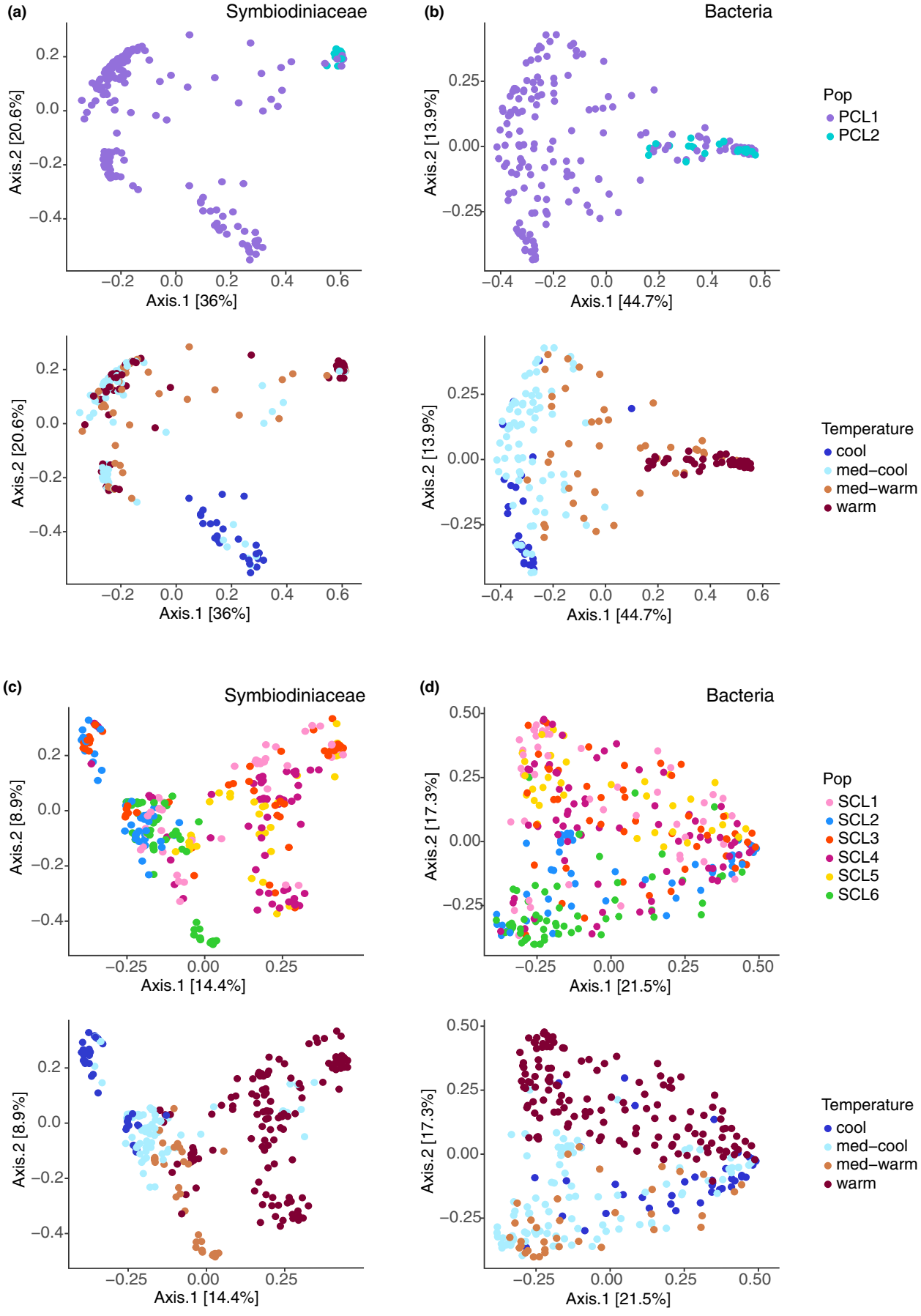

FIGURE 3 Microbiome (i.e., Symbiodiniaceae and prokaryotes) ordination plots based on Bray-Curtis dissimilarities. Individual colonies of (a, b) *P. verrucosa* and (c, d) *S. pistillata* are colored according to their population genetic cluster assignment and temperature regime (categorized by MMM). Percentage of variance explained by each axis is shown in bracket.

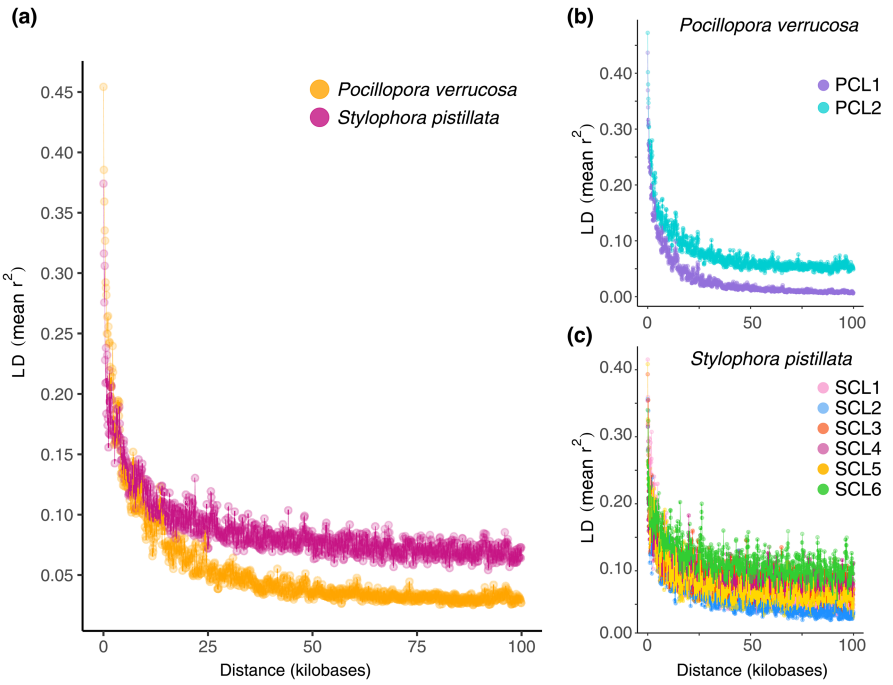

FIGURE 4 Decay of linkage disequilibrium (LD) as a function of physical distance between SNPs in *Pocillopora verrucosa* and *Stylophora pistillata*. (a) Overall LD decay for each species obtained from the average LD for each genetic population of (b) *P. verrucosa* and (c) *S. pistillata*. Each point represents the mean r^2 of bins of 100 bp.

assigned to one of the *K* genetic clusters (*P. verrucosa* = 203 colonies; *S. pistillata* = 312 colonies, see above). We used the same datasets of independent SNPs as for the population structure analyses (*P. verrucosa* = 35,208 SNPs; *S. pistillata* = 25,318 SNPs) for BAYESCAN and BAYPASS. We used these analyses to identify outlier SNPs showing significant divergence from neutrally behaving loci (higher than expected), indicative of positive diversifying selection. We detected 85 candidate SNPs indicative of positive selection in *P. verrucosa* compared to 128 in *S. pistillata*. Of these, 22 and 59 were commonly identified by BAYPASS and BAYESCAN for *P. verrucosa* and *S. pistillata*, respectively (Tables S17 and S18). The 85 candidate SNPs of *P. verrucosa* were distributed across 81 scaffolds and the 128 SNPs of *S. pistillata* were found across 120 scaffolds of the respective genome assemblies (Figure S12). Further inspection of candidate SNP allele frequencies in *P. verrucosa* showed that the majority of SNPs (*n* = 62) had less than 30% variation of allele frequencies between PCL1 and PCL2, including SNPs with alleles fixed at either genetic population (PCL1 = 19; PCL2 = 2). This low variation in allele frequencies between genetic populations is indicative of high gene flow (Weigand & Leese, 2018). However, it was surprising that SNPs exhibiting allele frequency changes between both populations were closer to fixation in PCL1 (*n* = 18) than in PCL2 (*n* = 5), as PCL2 is much more spatially and environmentally constrained. Changes in allele frequencies, indicative of fixed population differences, between *S. pistillata* populations revealed the highest number of fixed alleles in SCL5 (*n* = 32) and SCL2 (*n* = 27), corresponding to individuals from populations found exclusively in the southern and north-central Red Sea, respectively. The remaining populations showed lower numbers of fixed alleles in the order SCL1 (*n* = 20), SCL6 (*n* = 17), SCL3 (*n* = 16), and SCL4 (*n* = 4).

Given the rather rapid LD decay observed for both coral species (Figure 4), we followed a conservative approach by exploring adjacent genomic regions within 1 kb upstream and downstream of candidate SNPs (corresponding to a mean r^2 of ~0.25) to look for adaptively evolving candidate genes. Of the 85 *P. verrucosa* SNPs, 18 were in coding sequences (CDS), 21 SNPs were found in intronic regions, and 46 SNPs were located in intergenic regions (Table S17). Further, of the 18 SNPs found in coding sequences, eight SNPs were predicted to cause non-synonymous codon changes resulting in amino acid changes of genes involved in DNA repair, intracellular transport, cytoskeletal arrangement, transposons, and transcription factors, while one SNP was predicted to result in a stop codon, leading to a disrupted protein in a transmembrane receptor protein-tyrosine kinase involved in vascularization. Annotation of the 128 *S. pistillata* candidate SNPs showed that 24 were residing in a CDS, 54 in introns, and 50 in intergenic regions (Table S18). Of the 24 SNPs residing in a CDS, 14 were predicted to result in synonymous codon changes, while 10 SNPs were predicted to cause amino acid sequence changes of transmembrane transporters, transferases, and assembly of motile cilia (Table S18).

Irrespective of the site and type of change, we identified 40 and 84 genes with available functional annotation for the 85 and 128 SNPs considered across populations of *P. verrucosa* and *S. pistillata*, respectively. Functional inference using PANTHER identified metabolite interconversion enzymes as the protein class with the greatest representation in both species (*P. verrucosa* = 10; *S. pistillata* = 12) (Figure S13). Notably, some of these proteins have a role in the oxidative response to stress and lipid metabolism, arguably playing an important role in coral symbioses (Matthews et al., 2017; Rosic et al., 2014). For instance, peroxiredoxin found in *P. verrucosa* has been linked to the coral stress response to light, heat, and water quality (Levy et al., 2016; Tisthammer et al., 2021). Candidate genes were further assorted into the following protein classes: transporters (*P. verrucosa* = 1; *S. pistillata* = 7), protein-modifying enzymes

(*P. verrucosa* = 4; *S. pistillata* = 5), nucleic acid metabolism (*P. verrucosa* = 1; *S. pistillata* = 5), and protein-binding modulators (*P. verrucosa* = 1; *S. pistillata n* = 5) (Figure S13). Notably, several proteins are involved in cytoskeletal arrangement and ciliary function (e.g., target of rapamycin complex 2 subunit MAPKAP1, tubulin polyglutamylase, actin-related protein, myosin-Va, filamin-A), essential for nutrient and oxygen exchange (Pacherres et al., 2020), heterotrophic feeding (Brown & Bythell, 2005), horizontal microalgal symbiont acquisition (Harii et al., 2009), calcification (Tambutté et al., 2021), and heat stress (DeSalvo et al., 2008). Further extracellular matrix proteins such as collagen alpha chain, fibrillin-1, hemicentin, fibronectin type II domain, and fibropellin were identified and may be involved in biomineralization and tissue regeneration (Ba et al., 2015; Hemond et al., 2014; Reitzel et al., 2008; Takeuchi et al., 2016).

4 | DISCUSSION

Information on how genetic diversity is distributed across populations and prevailing environments is important to better understand how the protection of habitats can help species conservation efforts. In particular, the northern Red Sea has been coined a coral refuge with corals exhibiting thermal tolerances exceptionally higher than their local summer maxima (Evensen et al., 2021, 2022; Fine et al., 2013; Osman et al., 2018; Savary et al., 2021; Voolstra, Valenzuela, et al., 2021). To investigate patterns of genetic diversity and connectivity of Red Sea corals across their latitudinal spread, we assessed population genetic structure and signatures of selection in the common pocilloporid corals *P. verrucosa* and *S. pistillata*. In addition, we assessed patterns of Symbiodiniaceae and prokaryotic diversity, since microbiome assemblage contributes to coral holobiont biology (Osman et al., 2020; Rossbach et al., 2021; Voolstra, Suggett, et al., 2021; Ziegler, Seneca, et al., 2017).

4.1 | Greater connectivity of *P. verrucosa* versus complex structuring of *S. pistillata* suggest species-specific biogeography patterns and the absence of a common genetic break

Our study demonstrates that genetic diversity and holobiont structure of Red Sea coral populations differ between corals, even between species in the same family (i.e., Pocilloporidae) that are prevalent in the same reefs. Using a genome-wide RAD-Seq approach, we show that populations of *P. verrucosa* harbor a higher genetic variation and connectivity over the spread of the Red Sea than populations of *S. pistillata*, which are genetically less diverse and display a complex population structure. It is important to note that besides their phylogenetic relatedness, both species have contrasting reproductive modes (Shlesinger & Loya, 1985). The broadcast spawning coral *P. verrucosa* releases eggs and sperm into the water column for external fertilization, favoring the outcrossing of individuals and promoting long-distance dispersal (Bouwmeester et al., 2021; Robitzch et al., 2015), while fertilization of the brooding coral *S. pistillata* occurs internally, lowering outcrossing and often supporting high local recruitment (Ayre & Hughes, 2000; Rinkevich & Loya, 1979). This is further supported by our LD analysis, which shows a faster decay in populations of *P. verrucosa*. Thus, it appears that patterns of genetic diversity and differentiation are at least partially determined by the reproductive mode (Ayre & Hughes, 2000; Miller & Ayre, 2008). Similar findings have been previously reported for corals from the Great Barrier Reef (Thomas et al., 2014, 2020; Underwood et al., 2007) and the Western Indian Ocean (van der Ven et al., 2016, 2021). Nevertheless, LD is influenced by many factors, such as recombination rate, mutation rate, selection, drift, etc. (Slatkin, 2008). Thus, additional species should be studied to further ascertain the here-proposed relationship.

Although the prevailing environment clearly has a role in structuring coral microbial assemblage (discussed below), the notion of a common (host) genetic break at approximately 17–20° latitude that coincides with a marked environmental shift, as some studies have posited (Froukh & Kochzius, 2007; Giles et al., 2015; Nanninga et al., 2014; Saenz-Agudelo et al., 2015), is not supported by our data (DiBattista et al., 2020; Lim et al., 2020; Rossbach et al., 2021). Even in the case of *P. verrucosa*, where we identified (only) two genetic clusters (PCL1 and PCL2; Figure 2a), the population split is further south at about 16° latitude, while the remainder of the *P. verrucosa* Red Sea population constitutes a single population, as previously suggested (Robitzch et al., 2015). In comparison, the strong genetic differentiation of *S. pistillata* led to the identification of (at least) six genetic clusters (i.e., SCL1 to SCL6; Figure 2B, Figure S3B) with various degrees of connectivity across the Red Sea. Although the introgression among these clusters seems weak (as indicated by the at-large unanimous ancestry proportion of individuals to each genetic cluster, see Figure 2b coral host), many of the clusters are found in sympatry at the same reefs. This suggests a notable within-reef genetic differentiation, with colonies (i.e., genotypes) from different genetic clusters being represented at different sites, and thus, different genotypes being similarly successful under the same environmental settings (i.e., reef site). Genetic clusters of *S. pistillata* predominantly found in the southern region (i.e., SCL1, SCL3, SCL4, SCL5) were more related than those prevailing in the north-central region (i.e., SCL2, SCL6) (Figure 2b, Figure S3B). This regional prevalence denotes a shared demographic history among southern populations and suggests they might have evolved under similar selective pressures. In fact, the absence of bottleneck signatures such as inbreeding depression or lower genetic diversity in the southern reefs and the low levels of LD suggest long-term adaptation to the regional environment. Nevertheless, *S. pistillata* populations prevalent in the southern regions were not completely disconnected from the north-central Red Sea, arguing against a common barrier to gene flow (see above). Second, and most interestingly, the SCL3 genetic cluster present in the southern-most region can also be found in the northern-most region, and may explain the extraordinary thermal tolerance of corals from the Northern Red Sea and Gulf of Aqaba, thought to be due to historical selection, as corals passed through

the warmer southern Red Sea during recolonization from the Arabian Sea (Casazza, 2017; Fine et al., 2013). Conversely, the consistent low admixture levels between genetic clusters in *P. verrucosa* suggest introgression of the southern PCL2 into the northern and central PCL1 population, although the pattern is less clear. As such, our study provides the first genetic evidence linking northern- and southern-most Red Sea coral populations, which has been proposed as an explanation for the high bleaching threshold of northern Red Sea coral populations (Evensen et al., 2022; Fine et al., 2013; Osman et al., 2018; Voolstra, Valenzuela, et al., 2021). Importantly, however, this pattern is not universally applicable, but coral species-specific. Thus, other factors may need to be considered to fully resolve this phenomenon, e.g., microbial assemblage (Osman et al., 2020).

4.2 | Microbial assemblages are structured by host genotype and environmental regime

Surveying Symbiodiniaceae and prokaryotic diversity associated with *P. verrucosa* and *S. pistillata* using ITS2 and 16S marker gene sequencing, we found that microbial diversity patterns aligned with host genetic clusters and regional environmental regimes (here: MMM), although a causal link remains to be established. These results corroborate previous studies that posit that coral-associated microbial communities support acclimation to distinct thermal environments of the Red Sea (Osman et al., 2020; Rossbach et al., 2021; Voolstra, Valenzuela, et al., 2021), with a host genetic factor also being at play (Dubé et al., 2021). However, host genetic clusters partially align with the environmental gradient, at least in the case of *S. pistillata*. Thus, it is not straight-forward to disentangle the relative contribution, and a significant interaction between both factors (environment and host genotype) was found. Similarly, temperature gradients align with salinity and nutrient gradients, and cannot be fully resolved, which is why we refer to environmental regimes.

Symbiodiniaceae composition was coral species-specific. For *P. verrucosa*, it largely resembled the population genetic pattern of its coral host in that Symbiodiniaceae communities of *P. verrucosa* were largely consistent across the Red Sea except for the southern-most site where we also identified a distinct host genetic cluster. Notably, however, the northern-most sites (i.e., MAQ) showed a more variable Symbiodiniaceae assemblage that did not coincide with any distinct host genetic structure (Figures 2a and 3, Figure S5). By comparison, the *S. pistillata* Symbiodiniaceae assemblage at large was highly variable and regionally distinct to the extent that colonies from the same host genetic cluster in different regions associated with their regional-specific Symbiodiniaceae ITS2 profiles (Figures 2b and 3, Figure S5). Notably, coral-Symbiodiniaceae associations are not always host-specific or stable through time (e.g., after bleaching events). In the absence of time series data, we cannot unequivocally disentangle temporal stability of the observed host-symbiont associations (Hume et al., 2020).

At large, *P. verrucosa* and *S. pistillata* were associated with *Symbiodinium* ITS2 A1 algae as found previously (Hume et al., 2020; Voolstra, Valenzuela, et al., 2021; Ziegler, Arif, et al., 2017). Nevertheless, pronounced genetic differences exist, as evidenced by the multiple distinct ITS2 profiles, the significance of which remains to be determined (Voolstra, Valenzuela, et al., 2021). Both coral species were associated to a much lesser extent with *Cladocopium* spp. that was the dominant microalgal symbiont of *S. pistillata* in YAN-R1. In general, we observed an increasing frequency of *Cladocopium* association towards northern sites in both coral species, particularly ITS2 C1 in *P. verrucosa* and ITS2 C21 in *S. pistillata* (Figure S5). Similar patterns of increasing abundance of *Cladocopium* spp. associations with more northerly populations were observed previously for the giant clam *Tridacna maxima* (Rossbach et al., 2021) and the coral *P. verrucosa* (Sawall et al., 2014, 2015), supporting the notion that *Symbiodinium*- rather than *Cladocopium*-associations are better adapted to the southern Red Sea's warmer and nutrient-rich waters. While *Cladocopium* C1 has been documented in *Pocillopora* sp. from cooler reef regions (Brener-Raffalli et al., 2018; Ruiz Sebastián et al., 2009), the contrasting environmental regimes in which the Red Sea C1 associations are found, coupled with the known considerable genetic diversity harboured within the *Cladocopium* C1 radiation, mean that these two sets of C1 *Cladocopium* may be considerably genetically and phenotypically diverged. Notably, *P. verrucosa* typically hosts *Cladocopium* sp. across the Pacific Ocean at large, not *Symbiodinium*, which may provide further evidence to the argument that *Pocillopora-Symbiodinium* associations represent an adaptation to warmer and nutrient-rich waters (Johnston et al., 2022; Turnham et al., 2021). Although the Red Sea *P. verrucosa Cladocopium* C1 has been portrayed as a high-performance microalgal partner (Sawall et al., 2014, 2015), its association might be constrained to narrow environmental regimes. In light of this, one of the most interesting findings was the codominance of *Symbiodinium* and *Cladocopium* in both coral species in the Gulf of Aqaba sites (i.e., MAQ), a colder and more saline environment that nevertheless undergoes remarkable summer warming episodes of up to 15 Degree Heating Weeks (Osman et al., 2018). Corals in that region may have adapted to the unique environmentally challenging conditions through association with Symbiodiniaceae from both genera.

Similar to the Symbiodiniaceae patterns, prokaryotic assemblage patterns showed a coral species- and population-specific association that aligned with average seawater temperature differences (i.e., MMM) (Figure 3, Figure S9). For instance, microbiomes associated with populations of *S. pistillata* predominantly found in the south (SCL1, SCL3, SCL4, SCL5) were distinct from those found in the northern-central regions (SCL2 and SCL6). In line with this, the ASV indicator analysis revealed that most of the bacterial indicators were shared by clusters SCL1, SCL3, SCL4, SCL5 (Figure S10). Similarly, microbiomes associated with *P. verrucosa* were separated between PCL1 and PCL2 host genetic clusters (with some overlap) and clearly structured by the temperature regime (Figure 3). Interestingly, we identified a higher number of bacterial indicators for both coral species from the warmer southern regions, the majority of which belonged to the families Rhodobacteraceae, Flavobacteriaceae, and Endozoicomonadaceae (Figure S11; Table S16). Bacteria from

these families have previously been identified in pocilloporid microbiomes in the Red Sea (Bayer et al., 2013; Neave, Rachmawati, et al., 2017; Osman et al., 2020; Voolstra, Valenzuela, et al., 2021) and suggested to be functionally important for their coral host (Damjanovic et al., 2020; Neave et al., 2019; Neave, Michell, et al., 2017). While Rhodobacteraceae and Flavobacteriaceae were recently found to be associated with Symbiodiniaceae cells (Lawson et al., 2018; Maire et al., 2021), Endozoicomonadaceae represents a diverse family of gammaproteobacteria broadly associated with coral and marine invertebrates at large (Neave et al., 2016). On a global scale, it was found that *P. verrucosa* associates with the same *Endozoicomonas* types, whereas *Endozoicomonas* in *S. pistillata* were strongly grouped by geographic location (Neave, Rachmawati, et al., 2017). Here we observed a similar trend, but at a much smaller geographic scale. We could resolve 947 distinct 16S rRNA ASVs affiliated to Endozoicomonadaceae in both pocilloporid species. Of those, only a small fraction was specifically associated either with *P. verrucosa* (72 ASVs) or *S. pistillata* (103 ASVs), although species-specific Endozoicomonadaceae ASVs represented the most abundant ASVs. Interestingly, the majority of the coral-specific Endozoicomonadaceae associated with specific host genetic clusters, suggesting that some members of this group exhibit a high degree of phylosymbiosis (Pollock et al., 2018) and possibly functional specificity (Pogoreutz et al., 2022). Notably, this comprises genera other than *Endozoicomonas* in the family *Endozoicomonadaceae*. For instance, ASV0010 a member of the *Kistimonas* (*Endozoicomonadaceae*) was found almost exclusively in *S. pistillata* from the southernmost and northernmost reefs and was predominantly associated with host genetic cluster SCL3 that is prevalent in these regions. Taken together, our data show that prokaryotic association aligns with coral host genotype, Symbiodiniaceae identity, and the prevailing environment. This is reflected in the observed patterns of specificity and flexibility of prokaryotic assemblages as the product of phylosymbiotic constraints on the one hand and dynamic response to environmental conditions on the other hand (Pollock et al., 2018; Reshef et al., 2006; Voolstra & Ziegler, 2020).

4.3 | Candidate genes for positive selection and signatures of local adaptation in *P. verrucosa* and *S. pistillata*

We identified candidate genes under positive selection based on allele frequency changes between the identified genetic clusters in each coral species. In line with the lower genetic differentiation among the two *P. verrucosa* populations, differences in allele frequencies at candidate SNPs for positive selection were less distinct in *P. verrucosa*. We identified about half as many candidate genes in *P. verrucosa* as in *S. pistillata*, and the change in allele frequencies between the two genetic clusters was small, potentially owing to the high gene flow between both populations. Moreover, interpreting any putative adaptive advantage of *P. verrucosa* candidate genes was hampered by the fact that most of them had fixed (or close to fixed) SNP variants in the widely spread PCL1 population in comparison to the southernly constrained PCL2 cluster. This was unexpected as one might presume that the environmental conditions of the southern Red Sea would impose a stronger selective pressure leading to a high number of fixed variants in the PCL2 population. Among the positively selected candidate genes, we found many genes with a presumed function in countering environmental stress. Genes include the antioxidant peroxiredoxin that mitigates ROS (Levy et al., 2016; Tisthammer et al., 2021) and calmodulin, which has been proposed to prevent symbiont exocytosis under thermal stress (Weston et al., 2015). Further, we identified a Zinc metalloproteinase previously identified as a front-loaded gene in the coral heat stress response (Barshis et al., 2013; Voolstra, Valenzuela, et al., 2021). Interestingly, we identified several candidate genes that are putatively involved in coral ciliary function, possibly regulating nutrient exchange, heterotrophic feeding, and countering hypoxia (Pacherres et al., 2020; Shapiro et al., 2014). Further positive selection gene candidates, such as collagen alpha-2(I) chain precursor and fibrillin-1 were previously identified as targets of selection in *Acropora tenuis* from the Great Barrier Reef (Cooke et al., 2020).

Candidate genes for positive selection in *S. pistillata* were strongly supported by differences in allele frequencies among genetic clusters. Although the complex geographical distribution of the genetic clusters complicates the interpretation of the putative adaptive function in relation to the environment, we identified several candidate genes that exhibited fixed or near-fixed (≥98% allele frequency) SNP variants in genetic clusters prevalent in the north-central region compared to those prevalent in the south. Among these, we found translocating chain-associated membrane protein 1-like 1 (tram1l1), which has been associated with the response to hyposaline stress in the coral *Acropora millepora* (Aguilar et al., 2019). Likewise, mucopilin-3, a cation calcium regulated channel, is associated with osmomechanical stress (Jin et al., 2012). Because salinity decreases from north to south in the Red Sea, our finding may suggest that northern-migrated corals might have acquired adaptive features to compensate for osmotic disbalance in order to inhabit areas with higher salinity. At large, however, the finding of fixed variants in genes associated with the immune response, heat stress, and cell adhesion in genetic clusters prevalent in both the north-central and southern Red Sea suggests that coral adaptation is complex and detailed mechanistic studies are required to identify the particular adaptive benefit.

4.4 | Role of the environment in determining evolutionary trajectories and the need for multispecies investigations

Our study provides insight into the population genetic diversity and structure of two common pocilloporid corals across the Red Sea, highlighting differences at the holobiont level that suggest species-specific evolutionary trajectories. For the coral hosts, we found significant differences in their population genetic structure, suggesting

the absence of a common spatial genetic break as recently proposed (Nanninga et al., 2014). Rather, our data argue for the presence of species-specific biogeographic patterns that need to be considered for effective conservation of adaptively evolved genetic variants that may be critical for future survival. In the case of *P. verrucosa*, we found evidence for gene flow across sites that possibly ensures exchange of genetic material across the Red Sea. In contrast, *S. pistillata* exhibited distinct and fixed differences between sites that require the establishment of local protected areas for effective conservation of spatially variable alleles. Thus, corals exhibit species-specific evolutionary trajectories upon exposure to the same environmental regimes. The observed differences however align with differences in the reproductive mode, in line with long-established notions that brooding corals (such as *S. pistillata*) exhibit significant population differentiation in comparison to broadcast spawning corals (such as *P. verrucosa*) (Ayre & Hughes, 2000; Miller & Ayre, 2008). Importantly, however, the complex structure observed in *S. pistillata* contradicts a clear IBD pattern that is typically expected if brooders simply exhibit a lower dispersal range. Thus, other factors may need to be considered to fully explain the complex population genetic pattern. Further, and possibly explanatory, to the latter, we observed remarkable differences in microbial assemblage structured by host genetic diversity and the prevailing environment, arguably critical to coral biology, which may have to be factored into conservation strategies (Peixoto et al., 2022). Although *P. verrucosa* and *S. pistillata* are considered essential architects of coral reef environments, they only represent a small fraction of the Red Sea coral biodiversity (DeVantier et al., 2000). Consequently, future population genetic studies need to complement our understanding of genetic distribution patterns across coral genera and in relation to reproductive mode, prevailing environment, and life history (Darling et al., 2012). Notably, this is the first study to conduct a population genetic assessment of coral holobionts along the Saudi Arabian Red Sea coast, thus providing an important baseline against which to measure future genetic change. Our study adds to the growing body of large-scale Red Sea population genetic assessments, primarily focused on reef fish (DiBattista et al., 2020; Nanninga et al., 2014; Saenz-Agudelo et al., 2015), emphasizing the importance of multispecies investigations to inform the design of conservation areas to maximize genetic diversity and enhance the prospect of coral survival in the future.

AUTHOR CONTRIBUTIONS

Conceptualization: Carol Buitrago-López and Christian R. Voolstra. Sample collection: Yvonne Sawall. Data curation: Carol Buitrago-López, Thierry Gosselin, Anny Cardenas, Benjamin C. C. Hume, Fabian Staubach, and Christian R. Voolstra. Bioinformatic analysis: Carol Buitrago-López, Anny Cardenas, Benjamin C. C. Hume., and Thierry Gosselin. Interpretation: Carol Buitrago-López, Anny Cardenas, Benjamin C. C. Hume., Fabian Staubach, and Christian R. Voolstra. Funding acquisition: Christian R. Voolstra. Resources: Carol Buitrago-López, Daniel J. Barshis, Manuel Aranda, and Christian R. Voolstra. Supervision: Christian R. Voolstra. Validation: Carol Buitrago-Lóopez, Anny Cardenas, Benjamin C. C. Hume, and Christian R. Voolstra. Writing: Carol Buitrago-Lóopez, Anny Cardenas, Benjamin C. C. Hume, and Christian R. Voolstra. All authors reviewed and approved the final manuscript.

ACKNOWLEDGEMENTS

Research reported in this publication was supported by KAUST baseline research funds to CRV and the Deutsche Forschungsgemeinschaft (DFG, German Research Foundation) project number 433042944 to CRV. Open Access funding enabled and organized by Projekt DEAL. WOA Institution: UNIVERSITAET KONSTANZ.

CONFLICT OF INTEREST STATEMENT

The authors declare that no conflict of interest exists.

DATA AVAILABILITY STATEMENT

Sequencing data (RAD-Seq, ITS2, 16S) determined in this study have been made available under NCBI BioProject PRJNA805399 (https://www.ncbi.nlm.nih.gov/bioproject/PRJNA805399). The R and python scripts used to run analyses, statistics, and generate figures are available in the associated GitHub repository (https://github.com/reefgenomics/Red-Sea-RADSeq). ITS2-based Symbiodiniaceae clustered and non-clustered profile count tables are provided in the associated GitHub repository (https://github.com/reefgenomics/Red-Sea-RADSeq). 16S-based ASV relative abundance tables are provided in the associated GitHub repository (https://github.com/reefgenomics/Red-Sea-RADSeq).

ORCID

Carol Buitrago-López https://orcid.org/0000-0001-5985-5837
Anny Cárdenas https://orcid.org/0000-0002-4080-9010
Benjamin C. C. Hume https://orcid.org/0000-0001-7753-3903
Manuel Aranda https://orcid.org/0000-0001-6673-016X
Daniel J. Barshis https://orcid.org/0000-0003-1510-8375
Christian R. Voolstra https://orcid.org/0000-0003-4555-3795

REFERENCES

Aguilar, C., Raina, J.-B., Fôret, S., Hayward, D. C., Lapeyre, B., Bourne, D. G., & Miller, D. J. (2019). Transcriptomic analysis reveals protein homeostasis breakdown in the coral Acropora millepora during hyposaline stress. *BMC Genomics*, *20*(1), 148. https://doi.org/10.1186/s12864-019-5527-2

Alexander, D. H., & Lange, K. (2011). Enhancements to the ADMIXTURE algorithm for individual ancestry estimation. *BMC Bioinformatics*, *12*, 246. https://doi.org/10.1186/1471-2105-12-246

Allen, M. R., Dube, O. P., Solecki, W., Aragon-Durand, F., Cramer, W., Humphreys, S., & Zickfeld, K. (2018). *"Framing and Context" in Global Warming of 1.5 C: An IPCC Special Report on the impacts of global warming of 1.5 C above pre-industrial levels and related global greenhouse gas emission pathways, in the context of strengthening the global response to the threat of climate change, sustainable development, and efforts to eradicate poverty*. World Meteorological Organization.

Anderson, M. J., & Walsh, D. C. I. (2013). PERMANOVA, ANOSIM, and the Mantel test in the face of heterogeneous dispersions: What null hypothesis are you testing? *Ecological Monographs*, *83*(4), 557–574. https://doi.org/10.1890/12-2010.1

Andersson, A. F., Lindberg, M., Jakobsson, H., Bäckhed, F., Nyrén, P., & Engstrand, L. (2008). Comparative analysis of human gut microbiota by barcoded pyrosequencing. *PloS One*, *3*(7), e2836. https://doi.org/10.1371/journal.pone.0002836

Andrews, S. (2010). *FastQC: A quality control tool for high throughput sequence data [Online]*. http://www.bioinformatics.babraham.ac.uk/projects/fastqc/

Arrigoni, R., Benzoni, F., Terraneo, T. I., Caragnano, A., & Berumen, M. L. (2016). Recent origin and semi-permeable species boundaries in the scleractinian coral genus Stylophora from the Red Sea. *Scientific Reports*, *6*, 34612. https://doi.org/10.1038/srep34612

Ayre, D. J., & Hughes, T. P. (2000). Genotypic diversity and gene flow in brooding and spawning corals along the Great Barrier Reef, Australia. *Evolution*, *54*(5), 1590–1605. https://doi.org/10.1111/j.0014-3820.2000.tb00704.x

Ba, H., Yao, F., Yang, L., Qin, T., Luan, H., Li, Z., Zou, X., & Hou, L. (2015). Identification and expression patterns of extracellular matrix-associated genes fibropellin-ia and tenascin involved in regeneration of sea cucumber *Apostichopus japonicus*. *Gene*, *565*(1), 96–105. https://doi.org/10.1016/j.gene.2015.03.071

Baird, N. A., Etter, P. D., Atwood, T. S., Currey, M. C., Shiver, A. L., Lewis, Z. A., Selker, E. U., Cresko, W. A., & Johnson, E. A. (2008). Rapid SNP discovery and genetic mapping using sequenced RAD markers. *PloS One*, *3*(10), e3376. https://doi.org/10.1371/journal.pone.0003376

Barshis, D. J., Ladner, J. T., Oliver, T. A., Seneca, F. O., Traylor-Knowles, N., & Palumbi, S. R. (2013). Genomic basis for coral resilience to climate change. *Proceedings of the National Academy of Sciences of the United States of America*, *110*(4), 1387–1392. https://doi.org/10.1073/pnas.1210224110

Bay, R. A., & Palumbi, S. R. (2017). Transcriptome predictors of coral survival and growth in a highly variable environment. *Ecology and Evolution*, *7*(13), 4794–4803. https://doi.org/10.1002/ece3.2685

Bay, R. A., Rose, N. H., Logan, C. A., & Palumbi, S. R. (2017). Genomic models predict successful coral adaptation if future ocean warming rates are reduced. *Science Advances*, *3*(11), e1701413. https://doi.org/10.1126/sciadv.1701413

Bayer, T., Neave, M. J., Alsheikh-Hussain, A., Aranda, M., Yum, L. K., Mincer, T., Hughen, K., Apprill, A., & Voolstra, C. R. (2013). The microbiome of the Red Sea coral *Stylophora pistillata* is dominated by tissue-associated *Endozoicomonas* bacteria. *Applied and Environmental Microbiology*, *79*(15), 4759–4762. https://doi.org/10.1128/AEM.00695-13

Behr, A. A., Liu, K. Z., Liu-Fang, G., Nakka, P., & Ramachandran, S. (2016). pong: Fast analysis and visualization of latent clusters in population genetic data. *Bioinformatics*, *32*(18), 2817–2823. https://doi.org/10.1093/bioinformatics/btw327

Berumen, M. L., Voolstra, C. R., Daffonchio, D., Agusti, S., Aranda, M., Irigoien, X., Jones, B. H., Morán, X. A. G., & Duarte, C. M. (2019). The Red Sea: Environmental gradients shape a natural laboratory in a nascent ocean. In C. R. Voolstra & M. L. Berumen (Eds.), *Coral Reefs of the Red Sea* (pp. 1–10). Springer International Publishing. https://doi.org/10.1007/978-3-030-05802-9_1

Bolger, A. M., Lohse, M., & Usadel, B. (2014). Trimmomatic: A flexible trimmer for Illumina sequence data. *Bioinformatics*, *30*(15), 2114–2120. https://doi.org/10.1093/bioinformatics/btu170

Bourne, D. G., Morrow, K. M., & Webster, N. S. (2016). Insights into the Coral Microbiome: Underpinning the Health and Resilience of Reef Ecosystems. *Annual Review of Microbiology*, *70*, 317–340. https://doi.org/10.1146/annurev-micro-102215-095440

Bouwmeester, J., Coker, D. J., Sinclair-Taylor, T. H., & Berumen, M. L. (2021). Broadcast spawning of *Pocillopora verrucosa* across the eastern and western coast of the central Red Sea. *Ecosphere*, *12*(1), e03340. https://doi.org/10.1002/ecs2.3340

Brener-Raffalli, K., Clerissi, C., Vidal-Dupiol, J., Adjeroud, M., Bonhomme, F., Pratlong, M., Aurelle, D., Mitta, G., & Toulza, E. (2018). Thermal regime and host clade, rather than geography, drive Symbiodinium and bacterial assemblages in the scleractinian coral *Pocillopora damicornis* sensu lato. *Microbiome*, *6*(1), 39. https://doi.org/10.1186/s40168-018-0423-6

Brown, B. E., & Bythell, J. C. (2005). Perspectives on mucus secretion in reef corals. *Marine Ecology Progress Series*, *296*, 291–309. https://doi.org/10.3354/meps296291

Bruno, J. F., Selig, E. R., Casey, K. S., Page, C. A., Willis, B. L., Harvell, C. D., Sweatman, H., & Melendy, A. M. (2007). Thermal stress and coral cover as drivers of coral disease outbreaks. *PLoS Biology*, *5*(6), e124. https://doi.org/10.1371/journal.pbio.0050124

Buitrago-López, C., Mariappan, K. G., Cárdenas, A., Gegner, H. M., & Voolstra, C. R. (2020). The Genome of the Cauliflower Coral Pocillopora verrucosa. *Genome Biology and Evolution*, *12*(10), 1911–1917. https://doi.org/10.1093/gbe/evaa184

Callahan, B. J., McMurdie, P. J., Rosen, M. J., Han, A. W., Johnson, A. J. A., & Holmes, S. P. (2016). DADA2: High-resolution sample inference from Illumina amplicon data. *Nature Methods*, *13*(7), 581–583. https://doi.org/10.1038/nmeth.3869

Carricart-Ganivet, J. P., Cabanillas-Terán, N., Cruz-Ortega, I., & Blanchon, P. (2012). Sensitivity of calcification to thermal stress varies among genera of massive reef-building corals. *PloS One*, *7*(3), e32859. https://doi.org/10.1371/journal.pone.0032859

Casazza, L. R. (2017). Pleistocene reefs of the Egyptian Red Sea: Environmental change and community persistence. *PeerJ*, *5*, e3504. https://doi.org/10.7717/peerj.3504

Catchen, J., Hohenlohe, P. A., Bassham, S., Amores, A., & Cresko, W. A. (2013). Stacks: An analysis tool set for population genomics. *Molecular Ecology*, *22*(11), 3124–3140. https://doi.org/10.1111/mec.12354

Chattopadhyay, B., Garg, K. M., & Ramakrishnan, U. (2014). Effect of diversity and missing data on genetic assignment with RAD-Seq markers. *BMC Research Notes*, *7*, 841. https://doi.org/10.1186/1756-0500-7-841

Cingolani, P., Patel, V. M., Coon, M., Nguyen, T., Land, S. J., Ruden, D. M., & Lu, X. (2012). Using *Drosophila melanogaster* as a model for genotoxic chemical mutational studies with a new program, SnpSift. *Frontiers in Genetics*, *3*, 35. https://doi.org/10.3389/fgene.2012.00035

Cingolani, P., Platts, A., Wang, L. L., Coon, M., Nguyen, T., Wang, L., Land, S. J., Lu, X., & Ruden, D. M. (2012). A program for annotating and predicting the effects of single nucleotide polymorphisms, SnpEff: SNPs in the genome of *Drosophila melanogaster* strain w1118; iso-2; iso-3. *Fly*, *6*(2), 80–92. https://doi.org/10.4161/fly.19695

Combosch, D. J., & Vollmer, S. V. (2015). Trans-Pacific RAD-Seq population genomics confirms introgressive hybridization in Eastern Pacific Pocillopora corals. *Molecular Phylogenetics and Evolution*, *88*, 154–162. https://doi.org/10.1016/j.ympev.2015.03.022

Conway, J. R., Lex, A., & Gehlenborg, N. (2017). UpSetR: An R package for the visualization of intersecting sets and their properties. *Bioinformatics*, *33*(18), 2938–2940. https://doi.org/10.1093/bioinformatics/btx364

Cooke, I., Ying, H., Forêt, S., Bongaerts, P., Strugnell, J. M., Simakov, O., Zhang, J., Field, M. A., Rodriguez-Lanetty, M., Bell, S. C., Bourne, D. G., van Oppen, M. J., Ragan, M. A., & Miller, D. J. (2020). Genomic signatures in the coral holobiont reveal host adaptations driven by Holocene climate change and reef specific symbionts. *Science Advances*, *6*(48). https://doi.org/10.1126/sciadv.abc6318

D'Angelo, C., & Wiedenmann, J. (2014). Impacts of nutrient enrichment on coral reefs: New perspectives and implications for coastal management and reef survival. *Current Opinion in Environmental Sustainability*, *7*, 82–93. https://doi.org/10.1016/j.cosust.2013.11.029

Damjanovic, K., Menéndez, P., Blackall, L. L., & van Oppen, M. J. H. (2020). Early life stages of a common broadcast spawning coral associate with specific bacterial communities despite lack of

internalized bacteria. *Microbial Ecology*, *79*(3), 706–719. https://doi.org/10.1007/s00248-019-01428-1

Darling, E. S., Alvarez-Filip, L., Oliver, T. A., McClanahan, T. R., Côté, I. M., & Bellwood, D. (2012). Evaluating life-history strategies of reef corals from species traits. *Ecology Letters*, *15*(12), 1378–1386. https://doi.org/10.1111/j.1461-0248.2012.01861.x

Davies, S., Gamache, M. H., Howe-Kerr, L. I., Kriefall, N. G., Baker, A. C., Banaszak, A. T., Bay, L. K., Bellantuono, A. J., Bhattacharya, D., Chan, C. X., Claar, D. C., Coffroth, M. A., Cunning, R., Davy, S. K., del Campo, J., Diaz-Almeyda, E. M., Frommlet, J. C., Fuess, L. E., Gonzalez-Pech, R. A., … Parkinson, J. E. (2022). Building consensus around the assessment and interpretation of Symbiodiniaceae diversity. *Preprints*, 2022060284. https://doi.org/10.20944/preprints202206.0284.v1

De Cáceres, M., & Legendre, P. (2009). Associations between species and groups of sites: Indices and statistical inference. *Ecology*, *90*(12), 3566–3574. https://doi.org/10.1890/08-1823.1

DeSalvo, M. K., Voolstra, C. R., Sunagawa, S., Schwarz, J. A., Stillman, J. H., Coffroth, M. A., Szmant, A. M., & Medina, M. (2008). Differential gene expression during thermal stress and bleaching in the Caribbean coral Montastraea faveolata. *Molecular Ecology*, *17*(17), 3952–3971. https://doi.org/10.1111/j.1365-294X.2008.03879.x

DeVantier, L., Turak, E., Al-Shaikh, K., & De'ath, G. (2000). Coral communities of the central-northern Saudi Arabian Red Sea. *Fauna of Arabia*. *18*, 23–66. https://www.researchgate.net/profile/Lyndon-Devantier/publication/291213582_Coral_communities_of_the_central-northern_Saudi_Arabian_Red_Sea/links/56a68b6308ae997e22ba4a80/Coral-communities-of-the-central-northern-Saudi-Arabian-Red-Sea.pdf

DiBattista, J. D., Saenz-Agudelo, P., Piatek, M. J., Cagua, E. F., Bowen, B. W., Choat, J. H., Rocha, L. A., Gaither, M. R., Hobbs, J. A., Sinclair-Taylor, T. H., McIlwain, J. H., Priest, M. A., Braun, C. D., Hussey, N. E., Kessel, S. T., & Berumen, M. L. (2020). Population genomic response to geographic gradients by widespread and endemic fishes of the Arabian Peninsula. *Ecology and Evolution*, *10*(10), 4314–4330. https://doi.org/10.1002/ece3.6199

Dixon, G. B., Davies, S. W., Aglyamova, G. A., Meyer, E., Bay, L. K., & Matz, M. V. (2015). CORAL REEFS. Genomic determinants of coral heat tolerance across latitudes. *Science*, *348*(6242), 1460–1462. https://doi.org/10.1126/science.1261224

Donovan, M. K., Burkepile, D. E., Kratochwill, C., Shlesinger, T., Sully, S., Oliver, T. A., Hodgson, G., Freiwald, J., & van Woesik, R. (2021). Local conditions magnify coral loss after marine heatwaves. *Science*, *372*(6545), 977–980. https://doi.org/10.1126/science.abd9464

Dubé, C. E., Ziegler, M., Mercière, A., Boissin, E., Planes, S., Bourmaud, C. A.-F., & Voolstra, C. R. (2021). Naturally occurring fire coral clones demonstrate a genetic and environmental basis of microbiome composition. *Nature Communications*, *12*(1), 6402. https://doi.org/10.1038/s41467-021-26543-x

Eddy, T. D., Lam, V. W. Y., Reygondeau, G., Cisneros-Montemayor, A. M., Greer, K., Palomares, M. L. D., Bruno, J. F., Ota, Y., & Cheung, W. W. L. (2021). Global decline in capacity of coral reefs to provide ecosystem services. *One Earth*, *4*(9), 1278–1285. https://doi.org/10.1016/j.oneear.2021.08.016

Eren, A. M., Morrison, H. G., Lescault, P. J., Reveillaud, J., Vineis, J. H., & Sogin, M. L. (2015). Minimum entropy decomposition: Unsupervised oligotyping for sensitive partitioning of high-throughput marker gene sequences. *The ISME Journal*, *9*(4), 968–979. https://doi.org/10.1038/ismej.2014.195

Etter, P. D., Bassham, S., Hohenlohe, P. A., Johnson, E. A., & Cresko, W. A. (2011). SNP discovery and genotyping for evolutionary genetics using RAD sequencing. *Methods in Molecular Biology*, *772*, 157–178. https://doi.org/10.1007/978-1-61779-228-1_9

Evensen, N. R., Fine, M., Perna, G., Voolstra, C. R., & Barshis, D. J. (2021). Remarkably high and consistent tolerance of a Red Sea coral to acute and chronic thermal stress exposures. *Limnology and Oceanography*, *66*(5), 1718–1729. https://doi.org/10.1002/lno.11715

Evensen, N. R., Voolstra, C. R., Fine, M., Perna, G., Buitrago-López, C., Cárdenas, A., Banc-Prandi, G., Rowe, K., & Barshis, D. J. (2022). Empirically derived thermal thresholds of four coral species along the Red Sea using a portable and standardized experimental approach. *Coral Reefs*, *41*, 239–252. https://doi.org/10.1007/s00338-022-02233-y

Fine, M., Gildor, H., & Genin, A. (2013). A coral reef refuge in the Red Sea. *Global Change Biology*, *19*(12), 3640–3647. https://doi.org/10.1111/gcb.12356

Foll, M., & Gaggiotti, O. (2008). A genome-scan method to identify selected loci appropriate for both dominant and codominant markers: A Bayesian perspective. *Genetics*, *180*(2), 977–993. https://doi.org/10.1534/genetics.108.092221

Frieler, K., Meinshausen, M., Golly, A., Mengel, M., Lebek, K., Donner, S. D., & Hoegh-Guldberg, O. (2012). Limiting global warming to 2°C is unlikely to save most coral reefs. *Nature Climate Change*, *3*(2), 165–170. https://doi.org/10.1038/nclimate1674

Froukh, T., & Kochzius, M. (2007). Genetic population structure of the endemic fourline wrasse (*Larabicus quadrilineatus*) suggests limited larval dispersal distances in the Red Sea. *Molecular Ecology*, *16*(7), 1359–1367. https://doi.org/10.1111/j.1365-294X.2007.03236.x

Galili, T. (2015). dendextend: An R package for visualizing, adjusting and comparing trees of hierarchical clustering. *Bioinformatics*, *31*(22), 3718–3720. https://doi.org/10.1093/bioinformatics/btv428

Gautier, M. (2015). Genome-wide scan for adaptive divergence and association with population-specific covariates. *Genetics*, *201*(4), 1555–1579. https://doi.org/10.1534/genetics.115.181453

Giles, E. C., Saenz-Agudelo, P., Hussey, N. E., Ravasi, T., & Berumen, M. L. (2015). Exploring seascape genetics and kinship in the reef sponge Stylissa carteri in the Red Sea. *Ecology and Evolution*, *5*(13), 2487–2502. https://doi.org/10.1002/ece3.1511

Glynn, P. W. (1993). Coral reef bleaching: Ecological perspectives. *Coral Reefs*, *12*(1), 1–17. https://doi.org/10.1007/BF00303779

Gosselin, T. (2020). *thierrygosselin/radiator: Update*. https://doi.org/10.5281/zenodo.3687060

Gruber, B., Unmack, P. J., Berry, O. F., & Georges, A. (2018). dartr: An r package to facilitate analysis of SNP data generated from reduced representation genome sequencing. *Molecular Ecology Resources*, *18*(3), 691–699. https://doi.org/10.1111/1755-0998.12745

Harii, S., Yasuda, N., Rodriguez-Lanetty, M., Irie, T., & Hidaka, M. (2009). Onset of symbiosis and distribution patterns of symbiotic dinoflagellates in the larvae of scleractinian corals. *Marine Biology*, *156*(6), 1203–1212. https://doi.org/10.1007/s00227-009-1162-9

Hemond, E. M., Kaluziak, S. T., & Vollmer, S. V. (2014). The genetics of colony form and function in Caribbean Acropora corals. *BMC Genomics*, *15*, 1133. https://doi.org/10.1186/1471-2164-15-1133

Hughes, T. P., Anderson, K. D., Connolly, S. R., Heron, S. F., Kerry, J. T., Lough, J. M., Baird, A. H., Baum, J. K., Berumen, M. L., Bridge, T. C., Claar, D. C., Eakin, C. M., Gilmour, J. P., Graham, N. A. J., Harrison, H., Hobbs, J. A., Hoey, A. S., Hoogenboom, M., Lowe, R. J., … Wilson, S. K. (2018). Spatial and temporal patterns of mass bleaching of corals in the Anthropocene. *Science*, *359*(6371), 80–83. https://doi.org/10.1126/science.aan8048

Hughes, T. P., Kerry, J. T., Álvarez-Noriega, M., Álvarez-Romero, J. G., Anderson, K. D., Baird, A. H., Babcock, R. C., Beger, M., Bellwood, D. R., Berkelmans, R., Bridge, T. C., Butler, I. R., Byrne, M., Cantin, N. E., Comeau, S., Connolly, S. R., Cumming, G. S., Dalton, S. J., Diaz-Pulido, G., … Wilson, S. K. (2017). Global warming and recurrent mass bleaching of corals. *Nature*, *543*(7645), 373–377. https://doi.org/10.1038/nature21707

Hume, B., D'Angelo, C., Burt, J., Baker, A. C., Riegl, B., & Wiedenmann, J. (2013). Corals from the Persian/Arabian Gulf as models for thermotolerant reef-builders: Prevalence of clade C3 Symbiodinium, host fluorescence and ex situ temperature tolerance. *Marine Pollution Bulletin*, *72*(2), 313–322. https://doi.org/10.1016/j.marpolbul.2012.11.032

Hume, B. C. C., D'Angelo, C., Smith, E. G., Stevens, J. R., Burt, J., & Wiedenmann, J. (2015). Symbiodinium thermophilum sp. nov., a thermotolerant symbiotic alga prevalent in corals of the world's hottest sea, the Persian/Arabian Gulf. *Scientific Reports*, *5*, 8562. https://doi.org/10.1038/srep08562

Hume, B. C. C., Mejia-Restrepo, A., Voolstra, C. R., & Berumen, M. L. (2020). Fine-scale delineation of Symbiodiniaceae genotypes on a previously bleached central Red Sea reef system demonstrates a prevalence of coral host-specific associations. *Coral Reefs*, *39*(3), 583–601. https://doi.org/10.1007/s00338-020-01917-7

Hume, B. C. C., Smith, E. G., Ziegler, M., Warrington, H. J. M., Burt, J. A., LaJeunesse, T. C., Wiedenmann, J., & Voolstra, C. R. (2019). SymPortal: A novel analytical framework and platform for coral algal symbiont next-generation sequencing ITS2 profiling. *Molecular Ecology Resources*, *19*(4), 1063–1080. https://doi.org/10.1111/1755-0998.13004

Hume, B. C. C., Ziegler, M., Poulain, J., Pochon, X., Romac, S., Boissin, E., de Vargas, C., Planes, S., Wincker, P., & Voolstra, C. R. (2018). An improved primer set and amplification protocol with increased specificity and sensitivity targeting the Symbiodinium ITS2 region. *PeerJ*, *6*, e4816. https://doi.org/10.7717/peerj.4816

Jeffreys, H. (1939). The theory of probability. In *Oxford classic texts in the physical sciences*. Oxford University Press. https://global.oup.com/academic/product/the-theory-of-probability-9780198503682?cc=sa&lang=en&

Jin, M., Berrout, J., & O'Neil, R. G. (2012). Regulation of TRP channels by osmomechanical stress. In M. X. Zhu (Ed.), *TRP channels*. CRC Press/Taylor & Francis.

Johnston, E. C., Cunning, R., & Burgess, S. C. (2022). Cophylogeny and specificity between cryptic coral species (Pocillopora spp.) at Mo'orea and their symbionts (Symbiodiniaceae). *Molecular Ecology*, *31*(20), 5368–5385. https://doi.org/10.1111/mec.16654

Kamvar, Z. N., Tabima, J. F., & Grünwald, N. J. (2014). Poppr: An R package for genetic analysis of populations with clonal, partially clonal, and/or sexual reproduction. *PeerJ*, *2*, e281. https://doi.org/10.7717/peerj.281

Keshavmurthy, S., Yang, S.-Y., Alamaru, A., Chuang, Y.-Y., Pichon, M., Obura, D., Fontana, S., De Palmas, S., Stefani, F., Benzoni, F., MacDonald, A., Noreen, A. M., Chen, C., Wallace, C. C., Pillay, R. M., Denis, V., Amri, A. Y., Reimer, J. D., Mezaki, T., … Chen, C. A. (2013). DNA barcoding reveals the coral "laboratory-rat", Stylophora pistillata encompasses multiple identities. *Scientific Reports*, *3*, 1520. https://doi.org/10.1038/srep01520

Kleinhaus, K., Voolstra, C. R., Meibom, A., Amitai, Y., Gildor, H., & Fine, M. (2020). A closing window of opportunity to save a unique marine ecosystem. *Frontiers in Marine Science*, *7*, 1117. https://doi.org/10.3389/fmars.2020.615733

Kleypas, J., Allemand, D., Anthony, K., Baker, A. C., Beck, M. W., Hale, L. Z., Hilmi, N., Hoegh-Guldberg, O., Hughes, T., Kaufman, L., Kayanne, H., Magnan, A. K., Mcleod, E., Mumby, P., Palumbi, S., Richmond, R. H., Rinkevich, B., Steneck, R. S., Voolstra, C. R., … Gattuso, J.-P. (2021). Designing a blueprint for coral reef survival. *Biological Conservation*, *257*, 109107. https://doi.org/10.1016/j.biocon.2021.109107

LaJeunesse, T. C., Parkinson, J. E., Gabrielson, P. W., Jeong, H. J., Reimer, J. D., Voolstra, C. R., & Santos, S. R. (2018). Systematic revision of Symbiodiniaceae highlights the antiquity and diversity of coral endosymbionts. *Current Biology*, *28*(16), 2570–2580.e6. https://doi.org/10.1016/j.cub.2018.07.008

Langmead, B., & Salzberg, S. L. (2012). Fast gapped-read alignment with Bowtie 2. *Nature Methods*, *9*(4), 357–359. https://doi.org/10.1038/nmeth.1923

Lawson, C. A., Raina, J.-B., Kahlke, T., Seymour, J. R., & Suggett, D. J. (2018). Defining the core microbiome of the symbiotic dinoflagellate, Symbiodinium. *Environmental Microbiology Reports*, *10*(1), 7–11. https://doi.org/10.1111/1758-2229.12599

Lepais, O., & Weir, J. T. (2014). SimRAD: An R package for simulation-based prediction of the number of loci expected in RADseq and similar genotyping by sequencing approaches. *Molecular Ecology Resources*, *14*(6), 1314–1321. https://doi.org/10.1111/1755-0998.12273

Lesser, M. P. (2011). Coral bleaching: Causes and mechanisms. In *Coral reefs: An ecosystem in transition* (pp. 405–419). Springer. https://doi.org/10.1007/978-94-007-0114-4_23

Levy, O., Karako-Lampert, S., Waldman Ben-Asher, H., Zoccola, D., Pagès, G., & Ferrier-Pagès, C. (2016). Molecular assessment of the effect of light and heterotrophy in the scleractinian coral Stylophora pistillata. *Proceedings. Biological Sciences/The Royal Society*, *283*(1829). https://doi.org/10.1098/rspb.2015.3025

Li, H., Handsaker, B., Wysoker, A., Fennell, T., Ruan, J., Homer, N., Marth, G., Abecasis, G., Durbin, R., & 1000 Genome Project Data Processing Subgroup. (2009). The Sequence Alignment/Map format and SAMtools. *Bioinformatics*, *25*(16), 2078–2079. https://doi.org/10.1093/bioinformatics/btp352

Liew, Y. J., Aranda, M., & Voolstra, C. R. (2016). Reefgenomics.org – A repository for marine genomics data. *Database: The Journal of Biological Databases and Curation*, *2016*. https://doi.org/10.1093/database/baw152

Lim, K. K., Rossbach, S., Geraldi, N. R., Schmidt-Roach, S., Serrão, E. A., & Duarte, C. M. (2020). The Small Giant Clam, *Tridacna maxima* exhibits minimal population genetic structure in the red sea and genetic differentiation from the Gulf of Aden. *Frontiers in Marine Science*, *7*, 889. https://doi.org/10.3389/fmars.2020.570361

Liu, G., Heron, S. F., Eakin, C. M., Muller-Karger, F. E., Vega-Rodriguez, M., Guild, L. S., De La Cour, J. L., Geiger, E. F., Skirving, W. J., Burgess, T. F. R., Strong, A. E., Harris, A., Maturi, E., Ignatov, A., Sapper, J., Li, J., & Lynds, S. (2014). Reef-scale thermal stress monitoring of coral ecosystems: New 5-km global products from NOAA Coral Reef Watch. *Remote Sensing*, *6*(11), 11579–11606. https://doi.org/10.3390/rs61111579

Maier, E., Tollrian, R., & Nürnberger, B. (2009). Fine-scale analysis of genetic structure in the brooding coral Seriatopora hystrix from the Red Sea. *Coral Reefs*, *28*(3), 751–756. https://doi.org/10.1007/s00338-009-0497-5

Maier, E., Tollrian, R., Rinkevich, B., & Nürnberger, B. (2005). Isolation by distance in the scleractinian coral *Seriatopora hystrix* from the Red Sea. *Marine Biology*, *147*(5), 1109–1120. https://doi.org/10.1007/s00227-005-0013-6

Maire, J., Girvan, S. K., Barkla, S. E., Perez-Gonzalez, A., Suggett, D. J., Blackall, L. L., & van Oppen, M. J. H. (2021). Intracellular bacteria are common and taxonomically diverse in cultured and in hospite algal endosymbionts of coral reefs. *The ISME Journal*, *15*(7), 2028–2042. https://doi.org/10.1038/s41396-021-00902-4

Matthews, J. L., Crowder, C. M., Oakley, C. A., Lutz, A., Roessner, U., Meyer, E., Grossman, A. R., Weis, V. M., & Davy, S. K. (2017). Optimal nutrient exchange and immune responses operate in partner specificity in the cnidarian-dinoflagellate symbiosis. *Proceedings of the National Academy of Sciences of the United States of America*, *114*(50), 13194–13199. https://doi.org/10.1073/pnas.1710733114

Matz, M. V., Treml, E. A., Aglyamova, G. V., & Bay, L. K. (2018). Potential and limits for rapid genetic adaptation to warming in a Great Barrier Reef coral. *PLoS Genetics*, *14*(4), e1007220. https://doi.org/10.1371/journal.pgen.1007220

McMurdie, P. J., & Holmes, S. (2013). phyloseq: An R package for reproducible interactive analysis and graphics of microbiome census data. *PloS One*, *8*(4), e61217. https://doi.org/10.1371/journal.pone.0061217

Mi, H., Muruganujan, A., Ebert, D., Huang, X., & Thomas, P. D. (2019). PANTHER version 14: More genomes, a new PANTHER GO-slim and improvements in enrichment analysis tools. *Nucleic Acids Research*, *47*, D419–D426. https://doi.org/10.1093/nar/gky1038

Miller, K. J., & Ayre, D. J. (2008). Population structure is not a simple function of reproductive mode and larval type: Insights from tropical

corals. *The Journal of Animal Ecology*, *77*(4), 713–724. https://doi.org/10.1111/j.1365-2656.2008.01387.x

Moberg, F., & Folke, C. (1999). Ecological goods and services of coral reef ecosystems. *Ecological Economics*, *29*(2), 215–233. https://doi.org/10.1016/s0921-8009(99)00009-9

Monroe, A. (2015). *Genetic differentiation across multiple spatial scales of the Red Sea of the corals Stylophora pistillata and Pocillopora verrucosa*. https://doi.org/10.25781/KAUST-0U875

Muscatine, L., & Porter, J. W. (1977). Reef Corals: Mutualistic symbioses adapted to nutrient-poor environments. *Bioscience*, *27*(7), 454–460. https://doi.org/10.2307/1297526

Nanninga, G. B., Saenz-Agudelo, P., Manica, A., & Berumen, M. L. (2014). Environmental gradients predict the genetic population structure of a coral reef fish in the Red Sea. *Molecular Ecology*, *23*(3), 591–602. https://doi.org/10.1111/mec.12623

Neave, M. J., Apprill, A., Aeby, G., Miyake, S., & Voolstra, C. R. (2019). Microbial communities of Red Sea Coral Reefs. In C. R. Voolstra & M. L. Berumen (Eds.), *Coral Reefs of the Red Sea* (pp. 53–68). Springer International Publishing. https://doi.org/10.1007/978-3-030-05802-9_4

Neave, M. J., Apprill, A., Ferrier-Pagès, C., & Voolstra, C. R. (2016). Diversity and function of prevalent symbiotic marine bacteria in the genus *Endozoicomonas*. *Applied Microbiology and Biotechnology*, *100*(19), 8315–8324. https://doi.org/10.1007/s00253-016-7777-0

Neave, M. J., Michell, C. T., Apprill, A., & Voolstra, C. R. (2017). *Endozoicomonas* genomes reveal functional adaptation and plasticity in bacterial strains symbiotically associated with diverse marine hosts. *Scientific Reports*, *7*, 40579. https://doi.org/10.1038/srep40579

Neave, M. J., Rachmawati, R., Xun, L., Michell, C. T., Bourne, D. G., Apprill, A., & Voolstra, C. R. (2017). Differential specificity between closely related corals and abundant *Endozoicomonas* endosymbionts across global scales. *The ISME Journal*, *11*(1), 186–200. https://doi.org/10.1038/ismej.2016.95

Ngugi, D. K., Antunes, A., Brune, A., & Stingl, U. (2012). Biogeography of pelagic bacterioplankton across an antagonistic temperature-salinity gradient in the Red Sea. *Molecular Ecology*, *21*(2), 388–405. https://doi.org/10.1111/j.1365-294X.2011.05378.x

Novembre, J., Williams, R., Pourreza, H., Wang, Y., & Carbonetto, P. (2019). *PCAviz: Visualizing principal components analysis*. R package version 0.3-37. http://github.com/NovembreLab/PCAviz

Oksanen, J., Kindt, R., Legendre, P., O'Hara, B., Stevens, M. H. H., Oksanen, M. J., & Suggests, M. (2007). *The vegan package*. *Community ecology package*, *10*(631–637), 719. https://www.researchgate.net/profile/Gavin-Simpson-2/publication/228339454_The_vegan_Package/links/0912f50be86bc29a7f000000/The-vegan-Package.pdf

Osman, E. O., Smith, D. J., Ziegler, M., Kürten, B., Conrad, C., El-Haddad, K. M., Voolstra, C. R., & Suggett, D. J. (2018). Thermal refugia against coral bleaching throughout the northern Red Sea. *Global Change Biology*, *24*(2), e474–e484. https://doi.org/10.1111/gcb.13895

Osman, E. O., Suggett, D. J., Voolstra, C. R., Pettay, D. T., Clark, D. R., Pogoreutz, C., Sampayo, E. M., Warner, M. E., & Smith, D. J. (2020). Coral microbiome composition along the northern Red Sea suggests high plasticity of bacterial and specificity of endosymbiotic dinoflagellate communities. *Microbiome*, *8*(1), 8. https://doi.org/10.1186/s40168-019-0776-5

Pacherres, C. O., Ahmerkamp, S., Schmidt-Grieb, G. M., Holtappels, M., & Richter, C. (2020). Ciliary vortex flows and oxygen dynamics in the coral boundary layer. *Scientific Reports*, *10*(1), 1–10. https://doi.org/10.1038/s41598-020-64420-7

Palumbi, S. R., Barshis, D. J., Traylor-Knowles, N., & Bay, R. A. (2014). Mechanisms of reef coral resistance to future climate change. *Science*, *344*(6186), 895–898. https://doi.org/10.1126/science.1251336

Peixoto, R. S., Voolstra, C. R., Sweet, M., Duarte, C. M., Carvalho, S., Villela, H., Lunshof, J. E., Gram, L., Woodhams, D. C., Walter, J., Roik, A., Hentschel, U., Thurber, R. V., Daisley, B., Ushijima, B., Daffonchio, D., Costa, R., Keller-Costa, T., Bowman, J. S., … Berg, G. (2022). Harnessing the microbiome to prevent global biodiversity loss. *Nature Microbiology*, *7*, 1726–1735. https://doi.org/10.1038/s41564-022-01173-1

Pembleton, L. W., Cogan, N. O. I., & Forster, J. W. (2013). StAMPP: An R package for calculation of genetic differentiation and structure of mixed-ploidy level populations. *Molecular Ecology Resources*, *13*(5), 946–952. https://doi.org/10.1111/1755-0998.12129

Pinzón, J. H., Sampayo, E., Cox, E., Chauka, L. J., Chen, C. A., Voolstra, C. R., & LaJeunesse, T. C. (2013). Blind to morphology: Genetics identifies several widespread ecologically common species and few endemics among Indo-Pacific cauliflower corals (Pocillopora, Scleractinia). *Journal of Biogeography*, *40*(8), 1595–1608. https://doi.org/10.1111/jbi.12110

Pogoreutz, C., Oakley, C. A., Rädecker, N., Cárdenas, A., Perna, G., Xiang, N., Peng, L., Davy, S. K., Ngugi, D. K., & Voolstra, C. R. (2022). Coral holobiont cues prime Endozoicomonas for a symbiotic lifestyle. *The ISME Journal*, *16*, 1883–1895. https://doi.org/10.1038/s41396-022-01226-7

Pogoreutz, C., Rädecker, N., Cárdenas, A., Gärdes, A., Voolstra, C. R., & Wild, C. (2017). Sugar enrichment provides evidence for a role of nitrogen fixation in coral bleaching. *Global Change Biology*, *23*(9), 3838–3848. https://doi.org/10.1111/gcb.13695

Pollock, F. J., McMinds, R., Smith, S., Bourne, D. G., Willis, B. L., Medina, M., Thurber, R. V., & Zaneveld, J. R. (2018). Coral-associated bacteria demonstrate phylosymbiosis and cophylogeny. *Nature Communications*, *9*(1), 4921. https://doi.org/10.1038/s41467-018-07275-x

Prada, C., Hanna, B., Budd, A. F., Woodley, C. M., Schmutz, J., Grimwood, J., Iglesias-Prieto, R., Pandolfi, J. M., Levitan, D., Johnson, K. G., Knowlton, N., Kitano, H., DeGiorgio, M., & Medina, M. (2016). Empty niches after extinctions increase population sizes of modern corals. *Current Biology*, *26*(23), 3190–3194. https://doi.org/10.1016/j.cub.2016.09.039

Purcell, S., Neale, B., Todd-Brown, K., Thomas, L., Ferreira, M. A. R., Bender, D., Maller, J., Sklar, P., de Bakker, P. I., Daly, M. J., & Sham, P. C. (2007). PLINK: A tool set for whole-genome association and population-based linkage analyses. *American Journal of Human Genetics*, *81*(3), 559–575. https://doi.org/10.1086/519795

Quast, C., Pruesse, E., Yilmaz, P., Gerken, J., Schweer, T., Yarza, P., Peplies, J., & Glöckner, F. O. (2013). The SILVA ribosomal RNA gene database project: Improved data processing and web-based tools. *Nucleic Acids Research*, *41*, D590–D596. https://doi.org/10.1093/nar/gks1219

Rädecker, N., Pogoreutz, C., Gegner, H. M., Cárdenas, A., Roth, F., Bougoure, J., Guagliardo, P., Wild, C., Pernice, M., Raina, J.-B., Meibom, A., Voolstra, C. R., & Voolstra, C. R. (2021). Heat stress destabilizes symbiotic nutrient cycling in corals. *Proceedings of the National Academy of Sciences of the United States of America*, *118*(5). https://doi.org/10.1073/pnas.2022653118

Raitsos, D. E., Yi, X., Platt, T., Racault, M.-F., Brewin, R. J. W., Pradhan, Y., Papadopoulos, V. P., Sathyendranath, S., & Hoteit, I. (2015). Monsoon oscillations regulate fertility of the Red Sea. *Geophysical Research Letters*, *42*(3), 855–862. https://doi.org/10.1002/2014gl062882

Reitzel, A. M., Sullivan, J. C., Traylor-Knowles, N., & Finnerty, J. R. (2008). Genomic survey of candidate stress-response genes in the estuarine anemone Nematostella vectensis. *The Biological Bulletin*, *214*(3), 233–254. https://doi.org/10.2307/25470666

Reshef, L., Koren, O., Loya, Y., Zilber-Rosenberg, I., & Rosenberg, E. (2006). The coral probiotic hypothesis. *Environmental Microbiology*, *8*(12), 2068–2073. https://doi.org/10.1111/j.1462-2920.2006.01148.x

Rinkevich, B., & Loya, Y. (1979). The reproduction of the Red Sea Coral Stylophora pistillata. I. Gonads and Planulae. *Marine Ecology Progress Series*, *1*(2), 133–144.

Robitzch, V., Banguera-Hinestroza, E., Sawall, Y., Al-Sofyani, A., & Voolstra, C. R. (2015). Absence of genetic differentiation in the coral Pocillopora verrucosa along environmental gradients of the Saudi Arabian Red Sea. *Frontiers in Marine Science*, *2*, 1183. https://doi.org/10.3389/fmars.2015.00005

Rochette, N. C., Rivera-Colón, A. G., & Catchen, J. M. (2019). Stacks 2: Analytical methods for paired-end sequencing improve RADseq-based population genomics. *Molecular Ecology*, *28*(21), 4737–4754. https://doi.org/10.1111/mec.15253

Rosic, N., Ling, E. Y. S., Chan, C.-K. K., Lee, H. C., Kaniewska, P., Edwards, D., Dove, S., & Hoegh-Guldberg, O. (2014). Unfolding the secrets of coral–algal symbiosis. *The ISME Journal*, *9*(4), 844–856. https://doi.org/10.1038/ismej.2014.182

Rossbach, S., Hume, B. C. C., Cárdenas, A., Perna, G., Voolstra, C. R., & Duarte, C. M. (2021). Flexibility in Red Sea Tridacna maxima-Symbiodiniaceae associations supports environmental niche adaptation. *Ecology and Evolution*, *11*(7), 3393–3406. https://doi.org/10.1002/ece3.7299

Ruiz Sebastián, C., Sink, K. J., McClanahan, T. R., & Cowan, D. A. (2009). Bleaching response of corals and their Symbiodinium communities in southern Africa. *Marine Biology*, *156*(10), 2049–2062. https://doi.org/10.1007/s00227-009-1236-8

Saenz-Agudelo, P., Dibattista, J. D., Piatek, M. J., Gaither, M. R., Harrison, H. B., Nanninga, G. B., & Berumen, M. L. (2015). Seascape genetics along environmental gradients in the Arabian Peninsula: Insights from ddRAD sequencing of anemonefishes. *Molecular Ecology*, *24*(24), 6241–6255. https://doi.org/10.1111/mec.13471

Savary, R., Barshis, D. J., Voolstra, C. R., Cárdenas, A., Evensen, N. R., Banc-Prandi, G., Fine, M., & Meibom, A. (2021). Fast and pervasive transcriptomic resilience and acclimation of extremely heat tolerant coral holobionts from the northern Red Sea. *Proceedings of the National Academy of Sciences of the United States of America*, *118*, e2023298118.

Sawall, Y., & Al-Sofyani, A. (2015). Biology of Red Sea Corals: Metabolism, reproduction, acclimatization, and adaptation. In N. M. A. Rasul & I. C. F. Stewart (Eds.), *The Red Sea: The formation, morphology, oceanography and environment of a Young Ocean Basin* (pp. 487–509). Springer Berlin Heidelberg.

Sawall, Y., Al-Sofyani, A., Banguera-Hinestroza, E., & Voolstra, C. R. (2014). Spatio-temporal analyses of symbiodinium physiology of the coral *Pocillopora verrucosa* along large-scale nutrient and temperature gradients in the Red Sea. *PLoS ONE*, *9*, e103179. https://doi.org/10.1371/journal.pone.0103179

Sawall, Y., Al-Sofyani, A., Hohn, S., Banguera-Hinestroza, E., Voolstra, C. R., & Wahl, M. (2015). Extensive phenotypic plasticity of a Red Sea coral over a strong latitudinal temperature gradient suggests limited acclimatization potential to warming. *Scientific Reports*, *5*, 8940. https://doi.org/10.1038/srep08940

Schloss, P. D., Westcott, S. L., Ryabin, T., Hall, J. R., Hartmann, M., Hollister, E. B., Lesniewski, R. A., Oakley, B. B., Parks, D. H., Robinson, C. J., Sahl, J. W., Stres, B., Thallinger, G. G., Van Horn, D. J., & Weber, C. F. (2009). Introducing mothur: Open-source, platform-independent, community-supported software for describing and comparing microbial communities. *Applied and Environmental Microbiology*, *75*(23), 7537–7541. https://doi.org/10.1128/AEM.01541-09

Schmidt-Roach, S., Miller, K. J., Lundgren, P., & Andreakis, N. (2014). With eyes wide open: A revision of species within and closely related to the *Pocillopora damicornis* species complex (Scleractinia; Pocilloporidae) using morphology and genetics. *Zoological Journal of the Linnean Society*, *170*(1), 1–33. https://doi.org/10.1111/zoj.12092

Seutin, G., White, B. N., & Boag, P. T. (1991). Preservation of avian blood and tissue samples for DNA analyses. *Canadian Journal of Zoology*, *69*(1), 82–90. https://doi.org/10.1139/z91-013

Shapiro, O. H., Fernandez, V. I., Garren, M., Guasto, J. S., Debaillon-Vesque, F. P., Kramarsky-Winter, E., Vardi, A., & Stocker, R. (2014). Vortical ciliary flows actively enhance mass transport in reef corals. *Proceedings of the National Academy of Sciences of the United States of America*, *111*(37), 13391–13396. https://doi.org/10.1073/pnas.1323094111

Shlesinger, Y., & Loya, Y. (1985). Coral community reproductive patterns: Red Sea versus the Great Barrier Reef. *Science*, *228*(4705), 1333–1335. https://doi.org/10.1126/science.228.4705.1333

Slatkin, M. (2008). Linkage disequilibrium – understanding the evolutionary past and mapping the medical future. *Nature Reviews. Genetics*, *9*(6), 477–485. https://doi.org/10.1038/nrg2361

Smith, H., Epstein, H., & Torda, G. (2017). The molecular basis of differential morphology and bleaching thresholds in two morphs of the coral *Pocillopora acuta*. *Scientific Reports*, *7*(1), 10066. https://doi.org/10.1038/s41598-017-10560-2

Spalding, M., Burke, L., Wood, S. A., Ashpole, J., Hutchison, J., & Zu Ermgassen, P. (2017). Mapping the global value and distribution of coral reef tourism. *Marine Policy*, *82*, 104–113. https://doi.org/10.1016/j.marpol.2017.05.014

Sully, S., Burkepile, D. E., Donovan, M. K., Hodgson, G., & van Woesik, R. (2019). A global analysis of coral bleaching over the past two decades. *Nature Communications*, *10*(1), 1264. https://doi.org/10.1038/s41467-019-09238-2

Sultan, S. A. R., Ahmad, F., & El-Hassan, A. (1995). Seasonal variations of the sea level in the central part of the Red Sea. *Estuarine, Coastal and Shelf Science*, *40*(1), 1–8. https://doi.org/10.1016/0272-7714(95)90008-X

Takeuchi, T., Yamada, L., Shinzato, C., Sawada, H., & Satoh, N. (2016). Stepwise evolution of coral biomineralization revealed with genome-wide proteomics and transcriptomics. *PloS One*, *11*(6), e0156424. https://doi.org/10.1371/journal.pone.0156424

Tambutté, E., Ganot, P., Venn, A. A., & Tambutté, S. (2021). A role for primary cilia in coral calcification? *Cell and Tissue Research*, *383*(3), 1093–1102. https://doi.org/10.1007/s00441-020-03343-1

Thomas, L., Kendrick, G. A., Stat, M., Travaille, K. L., Shedrawi, G., & Kennington, W. J. (2014). Population genetic structure of the Pocillopora damicornis morphospecies along Ningaloo Reef, Western Australia. *Marine Ecology Progress Series*, *513*, 111–119. https://doi.org/10.3354/meps10893

Thomas, L., Rose, N. H., Bay, R. A., López, E. H., Morikawa, M. K., Ruiz-Jones, L., & Palumbi, S. R. (2018). Mechanisms of thermal tolerance in reef-building corals across a fine-grained environmental mosaic: Lessons from Ofu, American Samoa. *Frontiers in Marine Science*, *4*, 434. https://doi.org/10.3389/fmars.2017.00434

Thomas, L., Underwood, J. N., Adam, A. A. S., Richards, Z. T., Dugal, L., Miller, K. J., & Gilmour, J. P. (2020). Contrasting patterns of genetic connectivity in brooding and spawning corals across a remote atoll system in northwest Australia. *Coral Reefs*, *39*(1), 55–60. https://doi.org/10.1007/s00338-019-01884-8

Tisthammer, K. H., Timmins-Schiffman, E., Seneca, F. O., Nunn, B. L., & Richmond, R. H. (2021). Physiological and molecular responses of lobe coral indicate nearshore adaptations to anthropogenic stressors. *Scientific Reports*, *11*(1), 3423. https://doi.org/10.1038/s41598-021-82569-7

Turnham, K. E., Wham, D. C., Sampayo, E., & LaJeunesse, T. C. (2021). Mutualistic microalgae co-diversify with reef corals that acquire symbionts during egg development. *The ISME Journal*, *15*, 3271–3285. https://doi.org/10.1038/s41396-021-01007-8

Underwood, J. N., Smith, L. D., Van Oppen, M. J. H., & Gilmour, J. P. (2007). Multiple scales of genetic connectivity in a brooding coral on isolated reefs following catastrophic bleaching. *Molecular Ecology*, *16*(4), 771–784. https://doi.org/10.1111/j.1365-294X.2006.03187.x

van der Ven, R. M., Flot, J.-F., Buitrago-López, C., & Kochzius, M. (2021). Population genetics of the brooding coral Seriatopora hystrix reveals patterns of strong genetic differentiation in the Western Indian Ocean. *Heredity*, *126*(2), 351–365. https://doi.org/10.1038/s41437-020-00379-5

van der Ven, R. M., Triest, L., & De Ryck, D. J. R. (2016). *Population genetic structure of the stony coral Acropora tenuis shows high but variable connectivity in East Africa*. https://onlinelibrary.wiley.com/doi/abs/10.1111/jbi.12643?casa_token=TP2dCE_hP3oAAAAA:Ap0suuRDvzvqAZgpn5L3VZTQg6_zPVR9aMmRr_Y_3jW-qO62YSfaXLUmHwy2ZMdks1I1OXDX2ms-L60EPg

Voolstra, C. R., Buitrago-López, C., Perna, G., Cárdenas, A., Hume, B. C. C., Rädecker, N., & Barshis, D. J. (2020). Standardized short-term acute heat stress assays resolve historical differences in coral thermotolerance across microhabitat reef sites. *Global Change Biology*, *26*(8), 4328–4343. https://doi.org/10.1111/gcb.15148

Voolstra, C. R., Li, Y., Liew, Y. J., Baumgarten, S., Zoccola, D., Flot, J.-F., Tambutté, S., Allemand, D., & Aranda, M. (2017). Comparative analysis of the genomes of *Stylophora pistillata* and *Acropora digitifera* provides evidence for extensive differences between species of corals. *Scientific Reports*, *7*(1), 17583. https://doi.org/10.1038/s41598-017-17484-x

Voolstra, C. R., Perna, G., Cárdenas, A., Colin, L., Dörr, M. S., & Fiesinger, A. (2022). DNA preservation & DNA extraction protocol for field collection of coral samples suitable for host-, marker gene-, and metagenomics-based sequencing approaches. *Zenodo*. doi: https://doi.org/10.5281/ZENODO.6523533

Voolstra, C. R., Quigley, K. M., Davies, S. W., Parkinson, J. E., Peixoto, R. S., Aranda, M., Baker, A. C., Barno, A. R., Barshis, D. J., Benzoni, F., Bonito, V., Bourne, D. G., Buitrago-López, C., Bridge, T. C. L., Chan, C. X., Combosch, D. J., Craggs, J., Frommlet, J. C., Herrera, S., … Sweet, M. (2021). Consensus guidelines for advancing coral holobiont genome and specimen voucher deposition. *Frontiers in Marine Science*, *8*, 1029. https://doi.org/10.3389/fmars.2021.701784

Voolstra, C. R., Suggett, D. J., Peixoto, R. S., Parkinson, J. E., Quigley, K. M., Silveira, C. B., Sweet, M., Muller, E. M., Barshis, D. J., Bourne, D. G., & Aranda, M. (2021). Extending the natural adaptive capacity of coral holobionts. *Nature Reviews Earth & Environment*, *2*(11), 747–762. https://doi.org/10.1038/s43017-021-00214-3

Voolstra, C. R., Valenzuela, J. J., Turkarslan, S., Cárdenas, A., Hume, B. C. C., Perna, G., Buitrago-López, C., Rowe, K., Orellana, M. V., Baliga, N. S., Paranjape, S., Banc-Prandi, G., Bellworthy, J., Fine, M., Frias-Torres, S., & Barshis, D. J. (2021). Contrasting heat stress response patterns of coral holobionts across the Red Sea suggest distinct mechanisms of thermal tolerance. *Molecular Ecology*, *30*, 4466–4480. https://doi.org/10.1111/mec.16064

Voolstra, C. R., & Ziegler, M. (2020). Adapting with microbial help: Microbiome flexibility facilitates rapid responses to environmental change. *BioEssays: News and Reviews in Molecular, Cellular and Developmental Biology*, *42*(7), e2000004. https://doi.org/10.1002/bies.202000004

Wang, Y., Raitsos, D. E., Krokos, G., Gittings, J. A., Zhan, P., & Hoteit, I. (2019). Physical connectivity simulations reveal dynamic linkages between coral reefs in the southern Red Sea and the Indian Ocean. *Scientific Reports*, *9*(1), 16598. https://doi.org/10.1038/s41598-019-53126-0

Weigand, H., & Leese, F. (2018). Detecting signatures of positive selection in non-model species using genomic data. *Zoological Journal of the Linnean Society*, *184*(2), 528–583. https://doi.org/10.1093/zoolinnean/zly007

Weston, A. J., Dunlap, W. C., Beltran, V. H., Starcevic, A., Hranueli, D., Ward, M., & Long, P. F. (2015). Proteomics links the redox state to calcium signaling during bleaching of the scleractinian coral *Acropora microphthalma* on exposure to high solar irradiance and thermal stress. *Molecular & Cellular Proteomics*, *14*(3), 585–595. https://doi.org/10.1074/mcp.M114.043125

Zhan, P., Subramanian, A. C., Yao, F., & Hoteit, I. (2014). Eddies in the Red Sea: A statistical and dynamical study. *Journal of Geophysical Research, C: Oceans*, *119*(6), 3909–3925. https://doi.org/10.1002/2013jc009563

Zheng, X., Levine, D., Shen, J., Gogarten, S. M., Laurie, C., & Weir, B. S. (2012). A high-performance computing toolset for relatedness and principal component analysis of SNP data. *Bioinformatics*, *28*(24), 3326–3328. https://doi.org/10.1093/bioinformatics/bts606

Ziegler, M., Arif, C., Burt, J. A., Dobretsov, S., Roder, C., LaJeunesse, T. C., & Voolstra, C. R. (2017). Biogeography and molecular diversity of coral symbionts in the genus Symbiodinium around the Arabian Peninsula. *Journal of Biogeography*, *44*(3), 674–686. https://doi.org/10.1111/jbi.12913

Ziegler, M., Seneca, F. O., Yum, L. K., Palumbi, S. R., & Voolstra, C. R. (2017). Bacterial community dynamics are linked to patterns of coral heat tolerance. *Nature Communications*, *8*(1), 14213. https://doi.org/10.1038/ncomms14213

Zoccola, D., Ounais, N., Barthelemy, D., Calcagno, R., Gaill, F., Henard, S., Hoegh-Guldberg, O., Janse, M., Jaubert, J., Putnam, H., Salvat, B., Voolstra, C. R., & Allemand, D. (2020). The World Coral Conservatory (WCC): A Noah's ark for corals to support survival of reef ecosystems. *PLoS Biology*, *18*(9), e3000823. https://doi.org/10.1371/journal.pbio.3000823

SUPPORTING INFORMATION

Additional supporting information can be found online in the Supporting Information section at the end of this article.

How to cite this article: Buitrago-López, C., Cárdenas, A., Hume, B. C. C., Gosselin, T., Staubach, F., Aranda, M., Barshis, D. J., Sawall, Y., & Voolstra, C. R. (2023). Disparate population and holobiont structure of pocilloporid corals across the Red Sea gradient demonstrate species-specific evolutionary trajectories. *Molecular Ecology*, *32*, 2151–2173. https://doi.org/10.1111/mec.16871